

RESEARCH ARTICLE

SPECIAL ISSUE: CELL BIOLOGY OF THE IMMUNE SYSTEM

Pan-SHIP1/2 inhibitors promote microglia effector functions essential for CNS homeostasis

Chiara Pedicone¹, Sandra Fernandes^{1,*}, Otto M. Dungan^{2,*}, Shawn M. Dormann², Dennis R. Viernes², Arijit A. Adhikari², Lydia B. Choi², Ebbing P. De Jong³, John D. Chisholm^{2,†} and William G. Kerr^{1,2,4,†,§}

ABSTRACT

We show here that both SHIP1 (*Inpp5d*) and its paralog SHIP2 (*Inpp1*) are expressed at protein level in microglia. To examine whether targeting of SHIP paralogs might influence microglial physiology and function, we tested the capacity of SHIP1-selective, SHIP2-selective and pan-SHIP1/2 inhibitors for their ability to impact on microglia proliferation, lysosomal compartment size and phagocytic function. We find that highly potent pan-SHIP1/2 inhibitors can significantly increase lysosomal compartment size, and phagocytosis of dead neurons and amyloid beta (A β)_{1–42} by microglia *in vitro*. We show that one of the more-potent and water-soluble pan-SHIP1/2 inhibitors, K161, can penetrate the blood-brain barrier. Consistent with this, K161 increases the capacity of CNS-resident microglia to phagocytose A β and apoptotic neurons following systemic administration. These findings provide the first demonstration that small molecule modulation of microglia function *in vivo* is feasible, and suggest that dual inhibition of the SHIP1 and 2 paralogs can provide a novel means to enhance basal microglial homeostatic functions for therapeutic purposes in Alzheimer's disease and, possibly, other types of dementia where increased microglial function could be beneficial.

KEY WORDS: Alzheimer's disease, SH2-containing inositol phosphatases, SHIPi, beta-amyloid, Microglia, Phagocytosis

INTRODUCTION

Alzheimer's disease is the most prominent form of age-related dementia and, with an aging population, the numbers of those afflicted in the United States is anticipated to almost treble by 2050 to a total of 13.8 million adults (Taylor et al., 2017). This poses a substantial upcoming economic burden on U.S. society as well as other nations with aging populations (Wimo et al., 2017). The cause of Alzheimer's-related dementia remains elusive, with formation of inter-neuronal tau fragments or neuro-fibrillary tau tangles (NFT) and/or amyloid beta (A β) plaque formation in the CNS thought to contribute to neuronal death and, consequently, cognitive decline. Significant pharmaceutical efforts have been expended to develop therapeutics for Alzheimer's disease that limit inappropriate

production of the A β fragment A β ₄₂ from the A β precursor protein (APP) by the proteases β -secretase 1 (BACE1) and γ -secretase (Moussa-Pacha et al., 2019). In addition, monoclonal antibody therapies that target A β have been met with difficulties in showing efficacy in human trials (van Dyck, 2018). Thus, the clinical failure of BACE inhibitors and A β antibodies in Alzheimer's disease over the last decade has led us to question the causal role of amyloidosis in disease pathology and cognitive decline, and may even have spurred a shift in therapeutic focus towards targeting tauopathies (or tauons) (Moussa-Pacha et al., 2019; Hoskin et al., 2019). Confusion as to the causes and treatment of Alzheimer's disease has been further exacerbated by the recent re-designation of ~20% of older Alzheimer's disease patients as having a different type of dementia caused by TDP-43 proteinopathy, called limbic-predominant age-related TDP-43 encephalopathy (LATE) (Nelson et al., 2019). Moreover, inclusion of patients with TDP-43 proteinopathies in clinical trials of Alzheimer's disease therapies that targeted amyloid-related mechanisms of pathogenesis might have hampered the capacity of these trials to reach statistically valid conclusions concerning efficacy.

Despite the failure of clinical efforts that target A β production in the CNS, there remains considerable interest in modulating microglia function and/or differentiation as a means to reduce amyloidosis, remove dead or dying neurons and, possibly, even NFTs. This novel form of immunotherapy for Alzheimer's disease is likely to have inherent advantages relative to passive Alzheimer's disease immunotherapies, such as antibodies that target A β . This proposed role for microglial modification in Alzheimer's disease therapy flies in the face of decades of studies associating microglia with inflammatory processes that contribute to, rather than abrogate, pathology in the Alzheimer's disease brain (Hansen et al., 2018; Sarlus and Heneka, 2017). Indeed, microglia have been associated with pathological processes in Alzheimer's disease, including production of inflammatory cytokines that kill neurons directly or that promote the neurocytotoxic function of astrocytes, loss of neuronal synapses and promotion of NFTs. However, microglia are also known to have substantial homeostatic functions in the brain, which include pruning of synapses or phagocytic clearance of dead cells, cell debris and beta-amyloid deposits. In fact, the relative balance between these cellular states of microglia as Alzheimer's disease progresses is likely to be crucial to whether microglial function is helpful or harmful (Sarlus and Heneka, 2017) – in other words, the type of microglia that predominate is likely to be essential to whether Alzheimer's disease is present and its degree of severity. Recent studies from two groups have provided compelling evidence that the brain-resident microglia compartment may harbor different subsets of microglia (Wendeln et al., 2018; Keren-Shaul et al., 2017). Depending upon local or systemic signals these microglia could either promote inflammatory processes that are detrimental in Alzheimer's disease or homeostatic functions that are

¹Department of Microbiology & Immunology, SUNY Upstate Medical University, Syracuse, NY 13210, USA. ²Department of Chemistry, Syracuse University, Syracuse, NY 13210, USA. ³Proteomics and Mass Spectrometry Core Facility, SUNY Upstate Medical University, Syracuse, NY, 13210, USA. ⁴Department of Pediatrics, SUNY Upstate Medical University, Syracuse, NY 13210, USA.

*These authors contributed equally to this work

†These authors contributed equally to this work

§Author for correspondence (kerrw@upstate.edu)

id W.G.K., 0000-0002-4720-7135

beneficial (Wendeln et al., 2018; Keren-Shaul et al., 2017). Further support for the latter role has come from analyses of human Alzheimer's disease patients homozygous for the R47H SNP in the TREM2 gene (Guerreiro et al., 2013; Jonsson et al., 2012; Neumann and Daly, 2012). TREM2 is an important activating receptor that is expressed selectively by tissue macrophages and their CNS counterparts, the microglia (Hsieh et al., 2009), where it can promote metabolism, phagocytosis, cytokine expression and proliferation in these differentiated myeloid cells (Hsieh et al., 2009; Ulland et al., 2017; Jay et al., 2017). Murine models of TREM2 deficiency, when paired with transgenes that promote amyloidosis, have unequivocally demonstrated that microglia can play a homeostatic role by clearing amyloid deposits in the CNS to prevent or slow the development of pathologies related to Alzheimer's disease and loss of cognitive function (Wang et al., 2015, 2016; Ulland et al., 2017; Griuciu et al., 2019; Parhizkar et al., 2019). However, it should be noted that there is some discrepancy here, as studies that used a different TREM2 mouse mutant found that TREM2 deficiency protects from Alzheimer's disease within certain contexts (Jay et al., 2017, 2015).

Based on analyses of TREM2 loss-of-function (LOF) mutations in both humans and mice, we can have a fair degree of confidence that targeting of TREM2 expression and activity or distal signaling pathways that promote microglial homeostatic functions will be beneficial to treat Alzheimer's disease. To this end, TREM2 signaling is limited by SHIP1 through its SH2 domain-mediated recruitment to DAP12, a TREM2 receptor component (Peng et al., 2010). In addition SHIP1 is also recruited to and limits signaling via dectin1 (officially known as Clec7a), a C-type lectin receptor expressed by both macrophages and microglia (Blanco-Mendez et al., 2015). Dectin1 has been implicated in the preservation of microglia in a homeostatic state despite the pathogenic milieu that prevails in the amyloidogenic 5XFAD transgenic mouse model of Alzheimer's disease (Ulland et al., 2017). These studies imply SHIP1 to be a molecular target for immunotherapy of Alzheimer's disease by promoting microglial homeostatic functions and differentiation. In addition, SHIP1 influences signaling downstream of other receptors expressed by terminally differentiated myeloid cells including CSF1R (hereafter referred to as M-CSF-R), FCGR (hereafter referred to as FcγR), Kit, GCSFR and CCR2. Thus, SHIP1 limits signaling through key receptors (i.e. TREM2, CCR2, dectin1) that promote microglial survival and proliferation in the CNS (i.e. TREM2, dectin1), their ability to sense and phagocytose Aβ plaques (i.e. TREM2) (Ulland et al., 2017, 2015; Wang et al., 2015, 2016) as well as migration of peripheral monocyte-macrophages (i.e. mo-Mφ) and microglia in the CNS towards Aβ plaques (i.e. CCR2) (El Khoury et al., 2007; Hickman and El Khoury, 2010). The SHIP1 paralog, SHIP2, has also been shown to limit M-CSF-R and FcγR signaling (Bruhns et al., 2000; Segawa et al., 2017; Wang et al., 2004). Thus, SHIP1 and/or SHIP2 are considered to be potential molecular targets for an immunotherapeutic approach to treat Alzheimer's disease through modulation of normal homeostatic functions. This novel approach could also be combined with antibody therapies directed against Aβ, as microglia are likely to be needed to clear Aβ-antibody immune complexes. Further support to target SHIP1 comes from genome-wide association studies (GWAS) that have identified single nucleotide polymorphisms (SNPs) in the SHIP1 (i.e. *INPP5D*) gene linked to Alzheimer's disease risk, including the rs35349669 (rs669) SNP that is strongly associated with Alzheimer's disease (Ruiz et al., 2014; Zhang et al., 2016). In cohorts totaling ~74,000 individuals, the rs669T minor allele has been robustly associated

with Alzheimer's disease risk (odds ratio, 1.08), with a population attributable fraction of 4.6% with these patients exhibiting increased *INPP5D* expression in peripheral blood (Lambert et al., 2013). A second study found that an Alzheimer's disease-associated SNP in the *INPP5D* locus in a Japanese cohort is also associated with increased *INPP5D* mRNA expression (Yoshino et al., 2017). These studies suggest that increased SHIP1 synthesis or activity is deleterious in humans and, possibly, compromises key microglial functions.

Independent of its involvement in TREM2 and dectin1 signaling, SHIP1 may also have physiological functions whose inhibition might be beneficial in therapy of Alzheimer's disease. For instance, SHIP1 limits the production of CSF3 (hereafter referred to as G-CSF) *in vivo* (Hazen et al., 2009; Iyer et al., 2015). Administration of G-CSF, or its administration together with SCF, has been shown to reduce disease severity in multiple murine Alzheimer's disease models (Prakash et al., 2013; Jiang et al., 2010; Sanchez-Ramos et al., 2009; Tsai et al., 2007; Li et al., 2011). Improved cognitive function has also been observed in a pilot study where G-CSF was administered to Alzheimer's disease patients (Sanchez-Ramos et al., 2012).

Because SHIP1 and, in some instances, SHIP2 can be recruited to receptors that are crucial to determine macrophage and microglial survival and effector functions, we assessed different classes of small molecule SHIP inhibitors. These include the SHIP1-selective inhibitor 3AC (Brooks et al., 2010), the SHIP2-selective inhibitor AS1949490 (Suwa et al., 2009) and the pan-SHIP1 inhibitors K118 (Srivastava et al., 2016; Gumbleton et al., 2017) and K149 (Hoekstra et al., 2016; Gumbleton et al., 2017) as well as new, more-potent pan-SHIP1/2 inhibitors we have developed ourselves. Our findings herein provide the first demonstration that small molecules enhance microglial effector functions associated with maintaining homeostasis in the CNS and, thus, provide a platform to further develop this class of immunotherapeutics to treat Alzheimer's disease.

RESULTS

Microglia express both SHIP paralogs

Both SHIP1 and SHIP2 are expressed in terminally differentiated macrophages. There, they have the capacity to regulate signaling at several different receptors that dictate macrophage effector functions, chemotaxis or survival (Bruhns et al., 2000; Segawa et al., 2017; Sly et al., 2003; Wang et al., 2004; Kamen et al., 2008, 2007; Lioubin et al., 1996; Damen et al., 1996). However, to our knowledge there has been no description of whether one or both SHIP paralogs are expressed at protein level in microglia derived from an embryonic myelo-erythroid progenitor, rather than an adult hematopoietic stem cell (HSC), such as macrophages (Ginhoux et al., 2010). Thus, we examined whether SHIP1, SHIP2 or both proteins are expressed in primary microglia by using intracellular flow cytometry (icFlow) and monoclonal antibodies specifically recognizing SHIP1 or SHIP2 (Fig. 1A). We confirmed the validity of the icFlow assays for SHIP1 and SHIP2, by also performing western blot analysis of primary microglia *ex vivo*. This showed the expected SHIP1 and SHIP2 isoforms of the expected apparent molecular weight (Fig. 1B). In addition, the presence of both SHIP paralogs was confirmed by western blot analysis (Fig. 1B) of cell lysates prepared from two different clonal murine microglial cell lines – BV-2 cells derived by oncogenic transduction of microglia (Mazzolla et al., 1997) and spontaneously immortalized SIM-A9 cells (Nagamoto-Combs et al., 2014) (Fig. 1B). Using the icFlow assay for SHIP1, we also confirmed that SHIP1 is expressed in

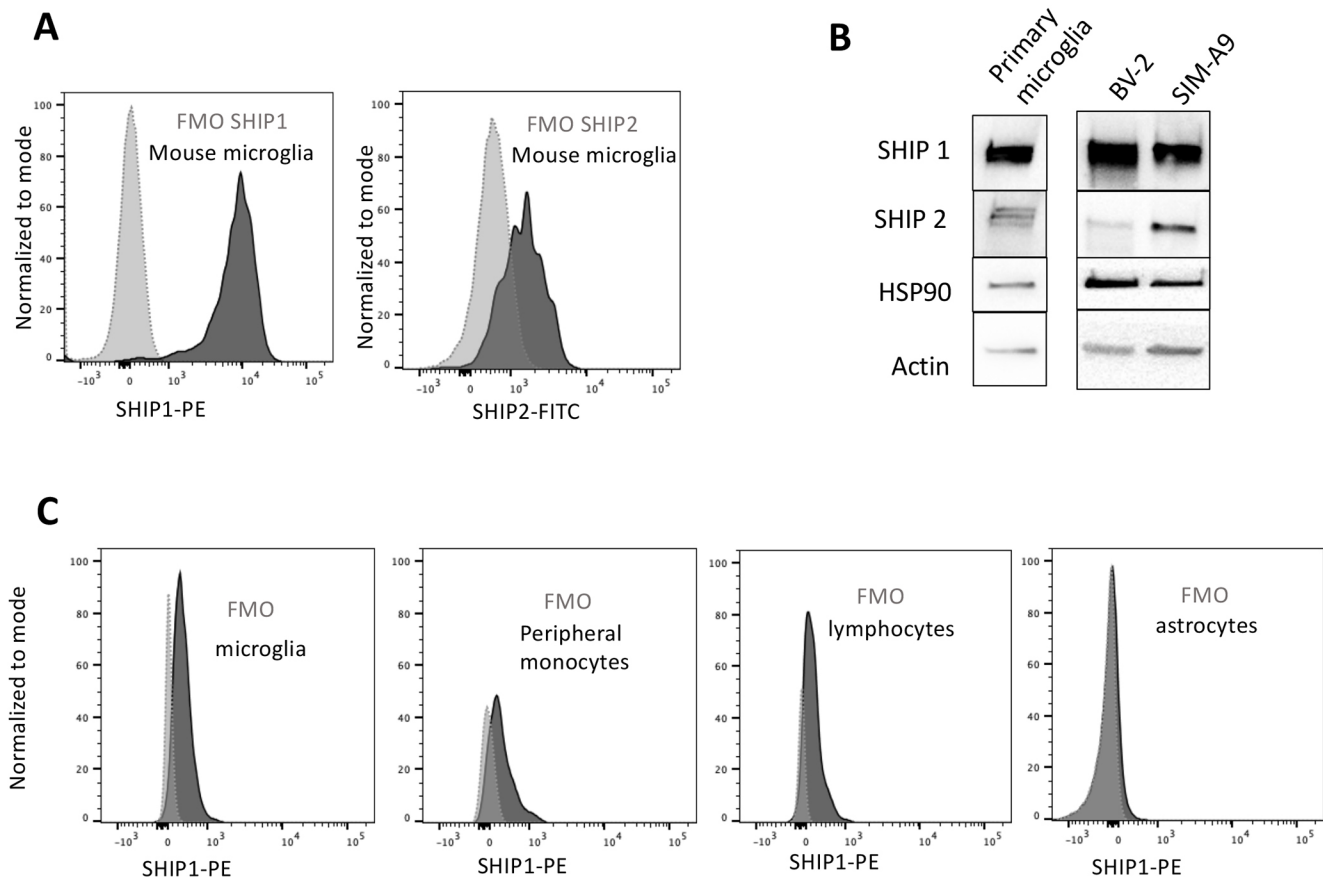


Fig. 1. Microglia express both SHIP paralogs. (A) Flow cytometry analysis of SHIP1 and SHIP2 expression in primary microglia compared to fluorescence minus one (FMO) on the same cells. (B) Western blot detection of SHIP1 and SHIP2 in primary microglia, BV-2 and SIM-A9. The two ubiquitously expressed proteins HSP90 and β -actin were used as internal control. (C) SHIP1 detection in the indicated brain cell population of adult mouse brain as identified by multi-parameter flow cytometry for CD11b, CD45 and ACSA2 (see example of multi-parameter flow cytometry in Fig. 7).

microglia of the adult CNS, as well as in peripheral leukocytes and monocytes that have entered the CNS; we did not detect SHIP1 protein expression in neuro-epithelial-derived astrocytes with this assay (Fig. 1C). SHIP1 and SHIP2 are then coexpressed in microglia; thus, each is potentially available for recruitment to receptors that regulate microglial homeostasis, phagocytosis and other effector functions.

Pan-SHIP1/2 inhibitors can promote proliferation of microglial cells *in vitro*

Both CSF1 (hereafter referred to as M-CSF) and IL34 are thought to renew and sustain the microglial compartment in the CNS via their common receptor M-CSF-R (Ginhoux et al., 2010; Kana et al., 2019; Greter et al., 2012; Alliot et al., 1999). SHIP1 and SHIP2 have been implied to regulate PI3K-mediated signaling via M-CSF-R in macrophages or osteoclasts, thereby promoting their growth and survival (Lioubin et al., 1996; Wang et al., 2004; Damen et al., 1996; Takeshita et al., 2002). We, therefore, sought to examine whether SHIP inhibitors promote proliferation of microglia *in vitro*. To test this, we compared the ability of SHIP1-selective inhibitor 3AC, SHIP2-selective inhibitor AS194940, and three pan-SHIP1/2 inhibitors K118, K149 and K161 to increase growth of BV-2 microglial cells *in vitro* (see Table S1 for structures, and the IC₅₀ values of SHIP1 and SHIP2 activity in response to all inhibitors). At low micromolar concentrations (1.25–5 μ M) only the pan-SHIP1/2 inhibitors K118, K161 and K149 significantly increased growth of BV-2 cells when compared with BV-2 cells treated with their

respective diluent controls (Fig. 2A). Across three independent experiments we found that, within the 2.5–5 μ M range, the pan-SHIP inhibitor K161 had the most potent and consistent impact on BV-2 microglial growth compared with SHIP1- and SHIP2-selective inhibitors. We further tested the effect of the different classes of SHIP inhibitors on cell growth in primary microglia. We found that the pan-SHIP1/2 inhibitor K161 also significantly improved primary microglia proliferation, whereas SHIP1-selective or SHIP2-selective inhibition (3AC and AS194940, respectively) did not (Fig. 2B). These findings indicate that pan-SHIP1/2 inhibitors have the potential to increase growth of microglia. Thus, this class of SHIP inhibitors merits further analysis regarding their impact on microglial homeostasis in both normal physiology and during pathogenesis.

Pan-SHIP1/2 inhibition promotes increases in lysosomal compartment size in microglia cell lines and primary microglia

The ability to phagocytose cell debris, dead or dying neurons and A β deposits within the CNS is an essential facet of microglial homeostatic function, and is dependent upon their lysosomal capacity or compartment size (Colonna and Butovsky, 2017). The lysosomal compartment has previously been thought to be a static subcellular organelle. However, it is now acknowledged to be a dynamic compartment that can respond to stress via PI3K-Akt-mTOR signaling that can be regulated by both SHIP1 and SHIP2 (Dibble and Cantley, 2015; Hipolito et al., 2018; Raben and

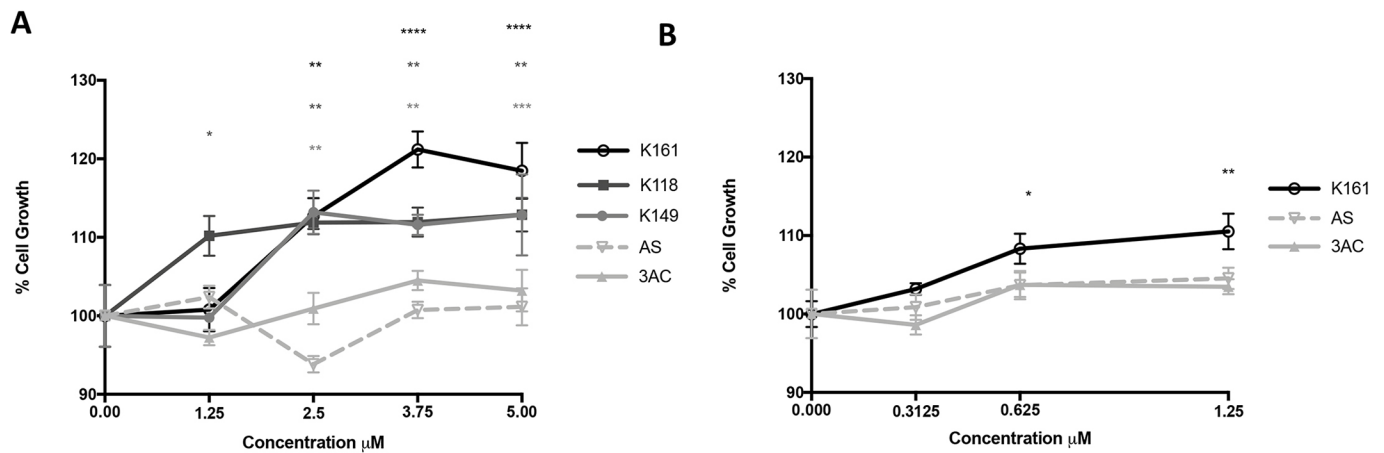


Fig. 2. Pan-SHIP1/2 inhibition increase proliferation of microglia *in vitro*. (A, B) A CCK-8 Dojindo assay was performed for analysis of cell growth of BV-2 cells (A) and primary microglia (B) treated with the SHIP inhibitors as indicated compared with that of their respective vehicle control (100%) at 48 h. Each point represents the mean of four replicates for each treatment. The experiment is representative of three independent experiments and was analyzed with two-way ANOVA. *P*-values are reported above each concentration of inhibitor when difference in cell growth was found to be significantly different than the diluent control. **P*<0.05, ***P*<0.01, ****P*<0.001, *****P*<0.0001. Error bars indicate the s.e.m.

Puertollano, 2016). To determine whether lysosomal compartment size is subject to dynamic control through SHIP enzymes, we analyzed the ability of different SHIP inhibitors to alter the size of the lysosomal compartment in microglia. We first analyzed lysosomal compartment size after treatment of BV-2 cells with the SHIP1-selective inhibitor 3AC, SHIP2-selective inhibitor AS194940 or pan-SHIP1/2 inhibitor K118 by using a diluent control (ethanol, ETOH). We found that both AS194940 and K118 promoted a significant expansion of lysosomal compartment size in BV-2 cells; however, K118 was demonstrably more potent in this effect than either diluent or AS194940 (Fig. 3A). As 3AC promoted no significant increase in lysosomal compartment size, we then focused on comparing AS194940 vs a panel of different pan-SHIP1/2 inhibitors and found that all pan-SHIP1/2 inhibitors tested promoted a robust increase in the lysosomal compartment size of BV-2 cells relative to either AS194940 or the diluent used (dimethyl sulfoxide, DMSO) (Fig. 3B). We also analyzed lysosomal compartment size in primary microglia after selective inhibition of SHIP1, SHIP2 or pan-SHIP1/2 (by, respectively, using 3AC, AS194940 or K161) and found a significant increase in lysosomal content only in the pan-SHIP inhibitor-treated cells [compared with vehicle-control (ETOH) cells; Fig. 3C]. To confirm that the increase in lysosomal compartment size promoted by pan-SHIP1/2 inhibition, observed by flow cytometry, corresponds, indeed, to an increase in the subcellular compartment, we also performed confocal microscopy of LysoTracker Red-stained BV-2 cells, and quantified intracellular staining by confocal image analysis. When compared to control vehicle-treated cells (DMSO), a significant increase in the size of lysosomal vesicular compartments was observed in BV-2 cells treated with pan-SHIP1/2 inhibitor K118 (Fig. 3D,E). These findings suggest that pan-SHIP1/2 inhibitors are the best choice of SHIP inhibitors in order to promote an increase in lysosomal capacity in microglia.

Pan-SHIP1/2 inhibition increases microglial phagocytosis of dead neurons

One of the essential homeostatic functions of microglia is to phagocytose dead and dying neurons in the CNS (Colonna and Butovsky, 2017). The SHIP1 and SHIP2 substrate phosphatidylinositol (3,4,5)-trisphosphate [PI(3,4,5)P₃] promotes initial events in the phagocytic process (Demirdjian et al., 2018;

Ostrowski et al., 2019) and SHIP1 has been shown to limit phagocytosis by macrophages (Kamen et al., 2008, 2007). To our knowledge macrophage phagocytic function has not been analyzed in SHIP2 knockout mice. Thus, we examined the different classes of SHIP inhibitors for their ability to enhance phagocytosis of dead neurons, whose nuclei were stained with propidium iodide (PI) to allow flow cytometric and confocal detection, and quantification of their phagocytosis. To examine this, microglia were incubated for 16 h with a SHIP inhibitor or diluent control and then for 2 h with dead neurons (5×10⁴/ml) before measuring uptake of dead neurons by flow cytometry. These experiments were initially performed in BV-2 cells, using the paralog selective inhibitors 3AC or AS194940, the pan-SHIP1/2 inhibitor K118, or a diluent (ethanol) as a control (Fig. 4A). Interestingly, only the pan-SHIP1/2 inhibitor K118 promoted a significant increase in the uptake of dead neurons compared with the diluent control. Thus, we repeated this analysis on BV-2 cells but, instead, used an expanded panel of pan-SHIP1/2 inhibitors, including some new ones with increased potency, and in some cases improved water solubility (see Table S1). All pan-SHIP1/2 inhibitors tested significantly increased phagocytosis of dead neurons, with K161 performing considerably better than other inhibitors (Fig. 4B). We repeated this experimental layout in SIM-A9 microglial cells and also found that all pan-SHIP1/2 inhibitors performed better than the diluent control, and with K161 also being the best pan-SHIP1/2 inhibitor of all five (Fig. 4C). We then confirmed that K161 enhances uptake of dead neurons by primary murine microglia (Fig. 4D) and human induced pluripotent stem cell (iPSC)-derived microglia (Fig. 4E). Furthermore, we confirmed by confocal microscopy image quantification that the increase in the uptake of dead neurons observed by flow cytometry was due to increased engulfment of dead neurons by K161-treated BV-2 microglia (Fig. 4F) and primary murine microglia (Fig. 4G). These findings establish that pan-SHIP1/2 inhibitors are best to enhance an essential microglial function, i.e. phagocytosis of dead neurons.

Pan-SHIP1/2 inhibition increase microglial phagocytosis of Aβ fragment 1-42

In addition to SHIP1 and SHIP2 playing a role in phagocytic and receptor-mediated endocytotic processes, SHIP1 can also be recruited to TREM2 (Peng et al., 2010). Thus, SHIP1, and possibly SHIP2, could be uniquely positioned to reduce PI(3,4,5)P₃ levels

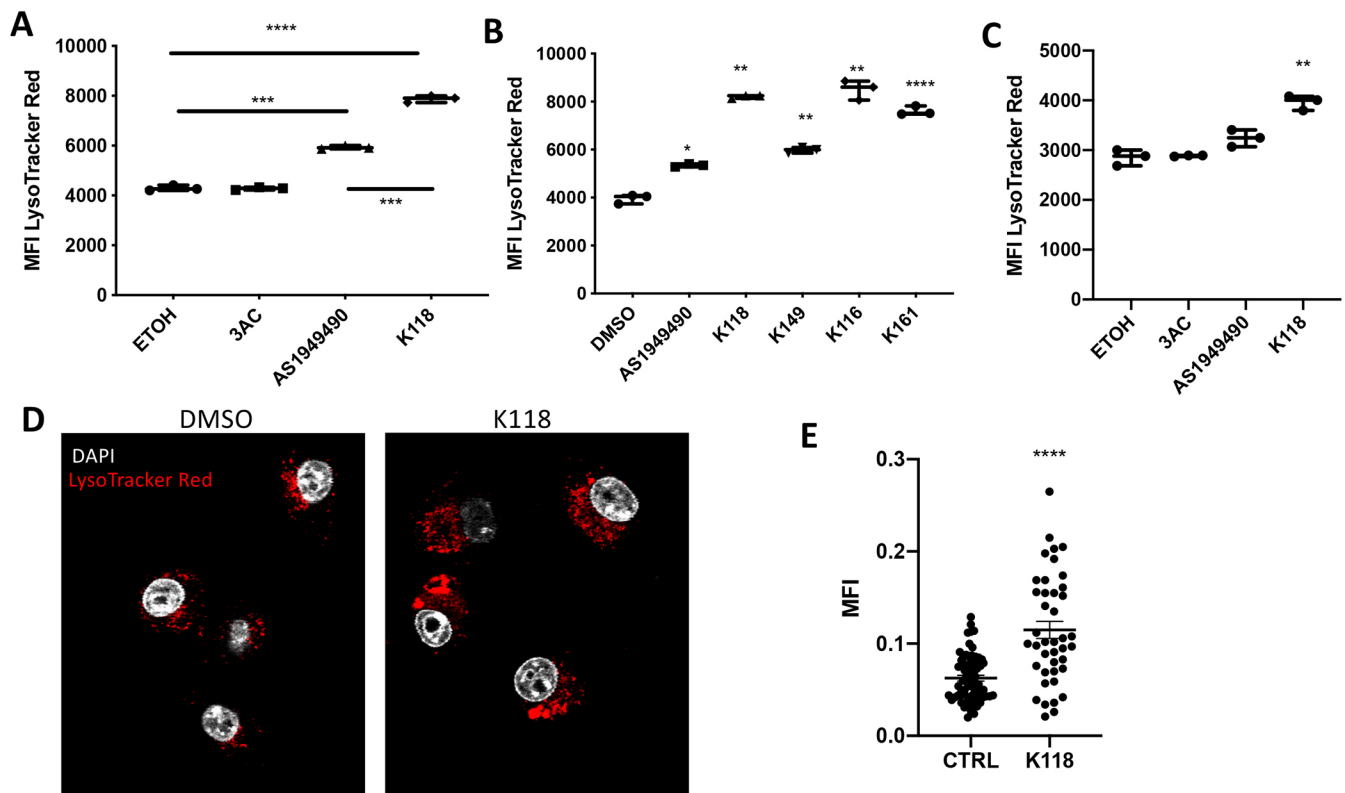


Fig. 3. Pan-SHIP1/2 inhibition increases microglial lysosomal compartment size. (A) Flow cytometry assay of LysoTracker Red staining on BV-2 cells treated for 16 h with the selective SHIP1 inhibitor (3AC), selective SHIP2 inhibitor (AS1949490) or the pan-SHIP1/2 inhibitor K118. (B) Flow cytometry assay of LysoTracker Red staining on BV-2 cells treated for 16 h with a panel of different pan-SHIP1/2 inhibitors (K118, K149, K116 and K161) at a concentration of 3.75 μ M. (C) LysoTracker Red-staining of primary murine microglia treated with 3AC, AS1949490 or K118 for 16 h. (D) Confocal image of fixed BV-2 cells after staining with LysoTracker Red (red channel) and DAPI (white channel) that show an increase in the lysosomal compartment of K118-treated versus diluent control. (E) Scatter plot showing the mean fluorescence intensity (MFI) of LysoTracker Red as determined by confocal microscopy image-analysis software. Each dot represents the fluorescent signal of an individual cell for its central z-stack plane. Each experiment is representative of three independent experiments. Statistical tests: Brown-Forsythe and Welch ANOVA (A,B,C), two-tailed *t*-test with Welch's correction (E). **P*<0.05, ***P*<0.01, ****P*<0.001, *****P*<0.0001. Error bars indicate min to max (A,B,C); s.e.m. (E).

when microglial cells initially engage and begin to interact with A β deposits for phagocytosis via TREM2 to reduce the efficiency of A β uptake. We hypothesized then that SHIP inhibitors also promote phagocytosis of the A β fragment 1-42 (A β ₁₋₄₂). To test this, we analyzed the ability of pan-SHIP1/2 inhibitors that performed well in the dead neuron phagocytosis assay above (i.e. K116, K118, K149 and K161) to influence the rate of phagocytosis. With the exception of K116, all pan-SHIP1/2 inhibitors tested significantly increased phagocytosis of A β ₁₋₄₂ by BV-2 microglia (Fig. 5A). As with phagocytosis of dead neurons by microglia, K161 appeared to enable optimal phagocytosis of A β ₁₋₄₂ in BV-2 cells. Thus, so we confirmed that K161 also promotes increased A β ₁₋₄₂ phagocytosis vs diluent control (H₂O) in primary microglia (Fig. 5B). The increased uptake of A β ₁₋₄₂-FITC promoted by K161 in BV-2 cells observed in our flow cytometry assay was thought to be due to intracellular uptake, which was confirmed by confocal microscopy (Fig. 5C). By using K118, we also measured A β ₁₋₄₂ phagocytosis at different times after exposure of BV-2 cells to A β ₁₋₄₂-FITC. K118 promoted a significant increase in A β ₁₋₄₂ uptake vs diluent controls as early as 30 min after exposure, with uptake plateauing between 1 h and 3 h after exposure to A β ₁₋₄₂ (Fig. 5E). In addition, K118 increased the overall capacity of BV-2 cells to phagocytose A β ₁₋₄₂ because at all three time-points of plateaued A β ₁₋₄₂ uptake, total uptake was significantly higher than in the diluent controls (Fig. 5E). Thus, pan-SHIP1/2 inhibition not only increased the

capacity of microglia to take up A β ₁₋₄₂ but also the efficiency of its uptake, which is consistent with SHIP enzymes reducing PI3K-generated PI(3,4,5)P₃ to reduce the efficiency of phagocytosis (Ostrowski et al., 2019; Kamen et al., 2008, 2007). We routinely observed that primary microglia were more sensitive to the effects of pan-SHIP1/2 inhibitors, like K161, such that improved proliferation, phagocytosis and increased lysosomal content are achieved with concentrations approximately two- to three-fold less than those required to achieve similar effects in transformed microglia lines. To verify that pan-SHIP1/2 inhibitor K161 is opposing PI3K signaling, we evaluated phosphorylation of AKT at serine 473, a key hallmark of PI3K signaling, in BV-2, SIMA9 and primary microglia treated with K161 or diluent, and found that a consistent and significant increase in Akt activation was promoted by K161 in microglia from all three cells (Fig. S1).

***In vivo* treatment with the pan-SHIP1/2 inhibitor K161 does not alter the frequency of the major cell populations in the CNS**

Our *in vitro* comparisons of different pan-SHIP1/2 inhibitors indicated that K161 is optimal for promoting phagocytic effector functions of microglia *in vitro*. We next sought to determine whether K161 is useful for improving these same effector functions of microglia after *in vivo* administration. Because microglia are a CNS-resident cell population that self-renews in the brain, it is

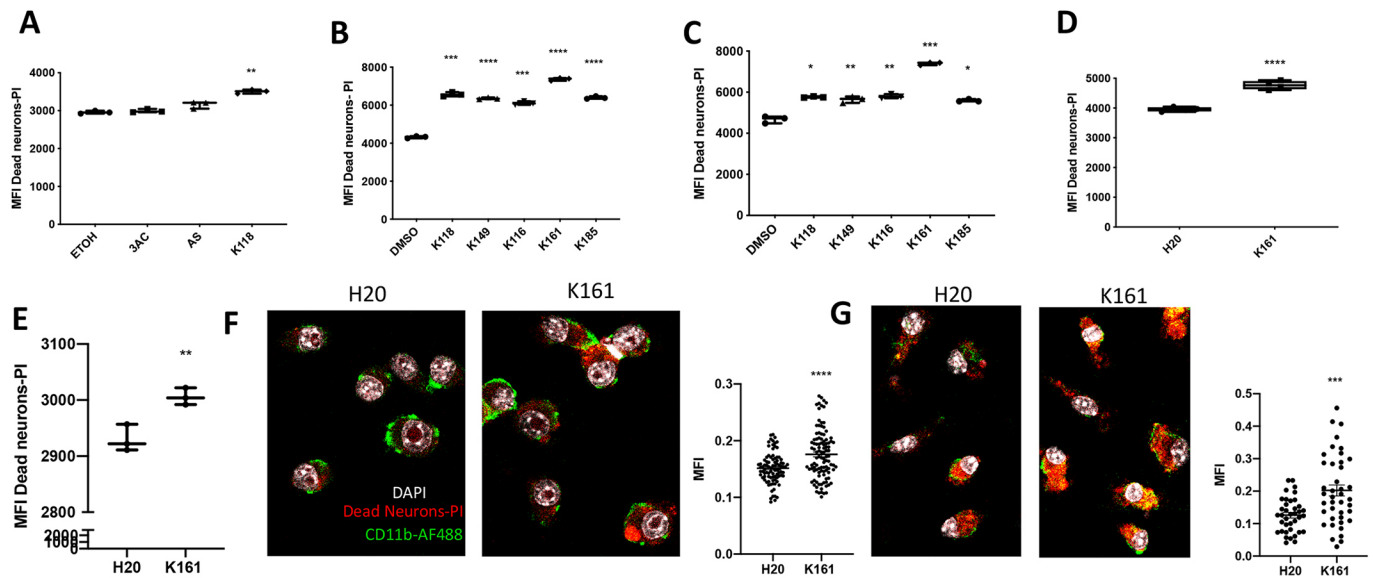


Fig. 4. Pan-SHIP1/2 inhibition increases the microglial phagocytosis of dead neurons. (A–E) Flow cytometric detection of dead neuron uptake by BV-2 cells (A,B), SIM-A9 cells (C), primary murine microglia (D) or human iPSC-derived microglia (E) treated for 16 h with the selective SHIP1 (3AC) or SHIP2 inhibitor (AS1949490), or a panel of pan-SHIP1/2 inhibitors (K118, K149, K116, K161 and K185) at a concentration of 3.75 μ M (BV-2 and SIMA-9) or 1.25 μ M (primary murine and human microglia) or their vehicle controls followed by incubation with apoptotic neurons for 2 h at 5×10^4 /ml. (F,G) Confocal images of dead neuron phagocytosis (red) by BV-2 cells (F) and primary murine microglia (G) followed by fixation and CD11b surface staining (green) and DAPI (white) to reveal microglial nuclei. To the right of each confocal image scatter plots of quantification for confocal microscopy images used for statistical analysis are shown. Each dot represents the fluorescence signal of an individual cell for its central z-stack plane. Statistical tests: Brown-Forsythe and Welch's ANOVA (A–C) or two-tailed *t*-test with Welch's correction (D–G). **P*<0.05, ***P*<0.01, ****P*<0.001, *****P*<0.0001. Error bars indicate min to max (A–E); s.e.m. (F,G).

unlikely that a compound incapable of penetrating the blood-brain barrier will impact microglial homeostasis and function. To assess the possibility of bioavailability of K161 in the CNS, mice were given a single dose of K161 either by oral gavage or intraperitoneal (i.p.) injection. We then harvested either serum (1, 4, 8, 12, 24 and 48 h post treatment) or the cerebral cortex (48 h post treatment) and processed both tissue samples for mass spectrometry detection of K161. We found that, with both routes of K161 administration, the inhibitor was present in the plasma within 1 h, declining significantly after 12 h regardless of the route of administration (Fig. 6A). Importantly, 48 h after dosing with K161 and independent of the route of administration, the inhibitor was readily detectable in the CNS at a concentration of ~ 20 –60 ng (Fig. 6B), indicating the bioavailability of K161 in the CNS. We then treated mice with K161 at 10 mg/kg (i.p.) twice a week for 3 weeks, harvested the cerebrum after perfusion and dissociated it. We then performed FACS analysis on the single-cell suspensions for CD11b, CD45 and ACSA2 which allowed detection of CD11b⁺CD45⁺ peripheral mo-M ϕ and CD11b⁺CD45^{low} microglia as well as CD45⁺CD11b⁻ leukocytes, CD11b⁻CD45⁻ neuroglial cells and CD11b⁻CD45⁻ACSA2⁺ astrocytes (Fig. 7A). Comparison of the frequency of these cell populations in the cerebrum of mice treated with K161 or vehicle showed that treatment of young WT mice with K161 did not significantly alter the frequency of any of these major cell populations or total CNS-infiltrating CD45⁺ cells (Fig. 7B). Increased surface expression of both CD11b and TREM2 has been linked to altered microglial activity, consistent with inflammatory behavior that may contribute to pathogenesis and disease progression in Alzheimer's disease – referred to as 'dark microglia' (Bisht et al., 2016). We also examined the mean surface density of both of these receptors and found that treatment with K161 did not significantly increase the density of either CD11b or TREM2 on the surface of microglia compared with vehicle (H₂O)-treated control mice (Fig. 7C).

Taken together these findings indicate K161 is able to access the CNS and, at least in young normal mice, does neither alter the homeostasis of major cell populations nor promote conversion of microglia to 'dark microglia'.

The capacity of CNS-resident microglia to phagocytose A β_{1-42} and dead neurons is increased by pan-SHIP1/2 inhibition *in vivo*

Our *in vitro* studies described above showed that K161 is able to promote increased lysosomal content and improved phagocytosis of both dead neurons and A β_{1-42} by microglia *in vitro*. Thus, in the same experiment described in Fig. 8, we also analyzed lysosomal content and phagocytic capacity of the cell populations present in the CNS of K161-treated mice and vehicle controls. We found that microglia in K161-treated mice have a higher capacity to phagocytose both A β_{1-42} and dead neurons (Fig. 8A,B); however, their lysosomal content remains unchanged compared with vehicle controls (Fig. 8C). Please note that the scale of the mean fluorescence intensity (MFI) values shown for each gated CNS cell population vary from one cell type to another. However, microglia have an inherently larger lysosomal compartment, and capacity to phagocytose dead neurons and A β_{1-42} relative to other cell populations in the CNS, including astrocytes – as would be expected for this professional phagocytic cell population in the CNS. Thus, the pan-SHIP1/2 inhibitor K161, consistent with its ability to enhance microglial phagocytic function *in vitro* and its ability to access the CNS, enhances microglial phagocytic functions *in vivo* that are crucial for CNS homeostasis.

DISCUSSION

The SH2-containing 5'-inositol phosphatases SHIP1 and SHIP2 have a unique role in the inositol phospholipid signaling pathway, as they can be recruited through their SH2 domains and other protein motifs to the plasma membrane, where they then convert

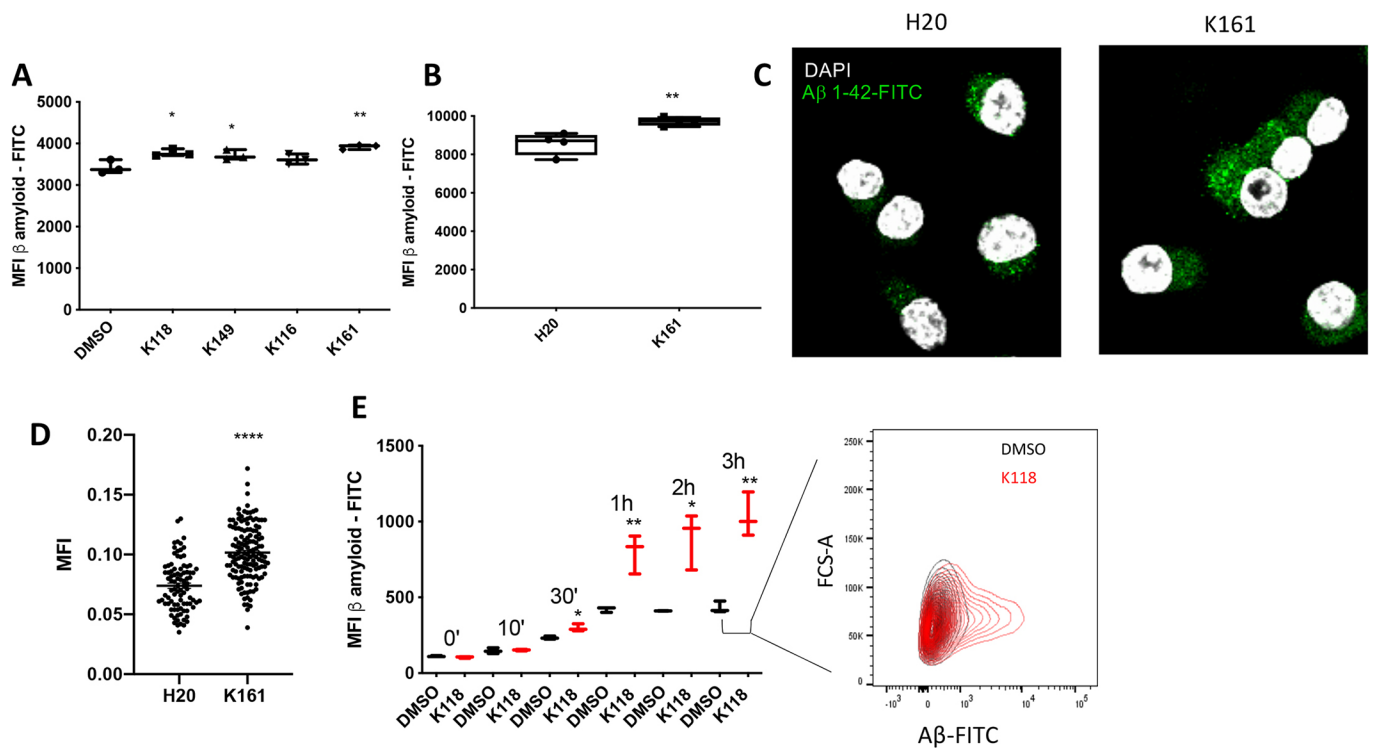


Fig. 5. Pan-SHIP1/2 inhibition increases the phagocytosis of A β ₁₋₄₂ peptide. (A,B) Flow cytometric measurement of A β ₁₋₄₂-FITC uptake by (A) BV-2 cells or (B) primary murine microglia after treatment for 16 h with the indicated pan-SHIP1/2 inhibitors at a concentration of 3.75 μ M (BV-2) or 1.25 μ M (primary microglia), or their respective vehicle controls (DMSO, BV-2; H₂O, primary microglia) followed by incubation for 1 h with 0.5 μ g/ml of A β ₁₋₄₂-FITC. (C) Representative confocal microscopy images of fixed BV-2 with A β ₁₋₄₂-FITC (green channel) and DAPI (white channel) show an increase of intracellular A β ₁₋₄₂-FITC uptake in the K161-treated cells versus the diluent control. (D) Scatter plots showing quantification of confocal microscopy images used for statistical analysis. Each dot represents the fluorescent signal of an individual cell for its central z-stack plane. (E) Kinetic analysis of A β ₁₋₄₂-FITC uptake by flow cytometry on BV-2 cells, and representative contour plots of BV-2 cells after incubation for 3 h with A β ₁₋₄₂-FITC shows a subpopulation of microglia have taken up a greater quantity of A β ₁₋₄₂-FITC relative to the diluent control. Statistical tests: Brown-Forsythe and Welch's ANOVA (A,E) or two-tailed *t*-test with Welch's correction (B,D). **P*<0.05, ***P*<0.01, *****P*<0.0001. Error bars indicate min to max (A,B,E); s.e.m. (D).

the PI 3-kinase product PI(3,4,5)P₃ to phosphatidylinositol (3,4)-bisphosphate [PI(3,4)P₂]. The latter, like PI(3,4,5)P₃, also has potent signaling properties, including the ability to activate Akt in cancer cells (Kerr, 2011). Here, we have shown *in vitro* and *in vivo* that microglia express both SHIP paralogs at the protein level. Moreover, we found that compounds that potentially inhibit both SHIP paralogs can significantly increase lysosomal capacity and phagocytosis through microglia *in vitro*. Importantly, K161, one of

the most-potent pan-SHIP1/2 inhibitors that emerged from our *in vitro* screening efforts, was able to increase the capacity of CNS-resident microglia to phagocytose both dead neurons and A β ₄₂ – the A β fragment thought to promote plaque formation and tissue pathology in Alzheimer's disease. Consistent with the impact of K161 on phagocytic functions of CNS-resident microglia, we showed that, following systemic administration, K161 penetrates the blood-brain barrier and is present in the cerebral cortex.

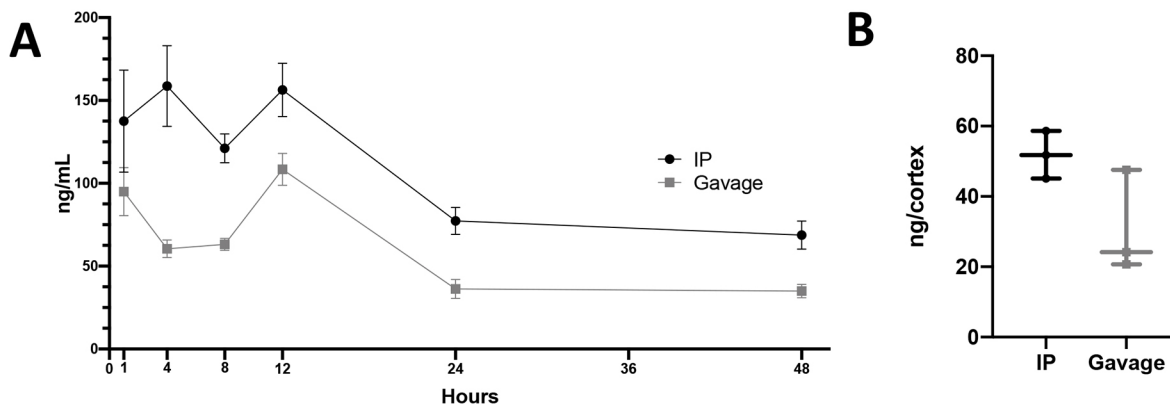


Fig. 6. Pharmacokinetics data of K161 levels in blood and brain from BL6 mice. (A,B) Mass spectrometry quantification of K161 levels in either the blood plasma (A; [ng/ml]) or the cerebral cortex (B [ng/cortex]) calculated as ng of K161 in the total cortex, after i.p. injection or oral gavage of the inhibitor. Blood was harvested and the concentration of K161 measured at times after treatment with K161 as indicated in A (*n*=6/group) or 48 h after treatment with K161 for cerebral cortex samples in B (*n*=3/group). Error bars indicate the s.e.m. (A), min to max (B).

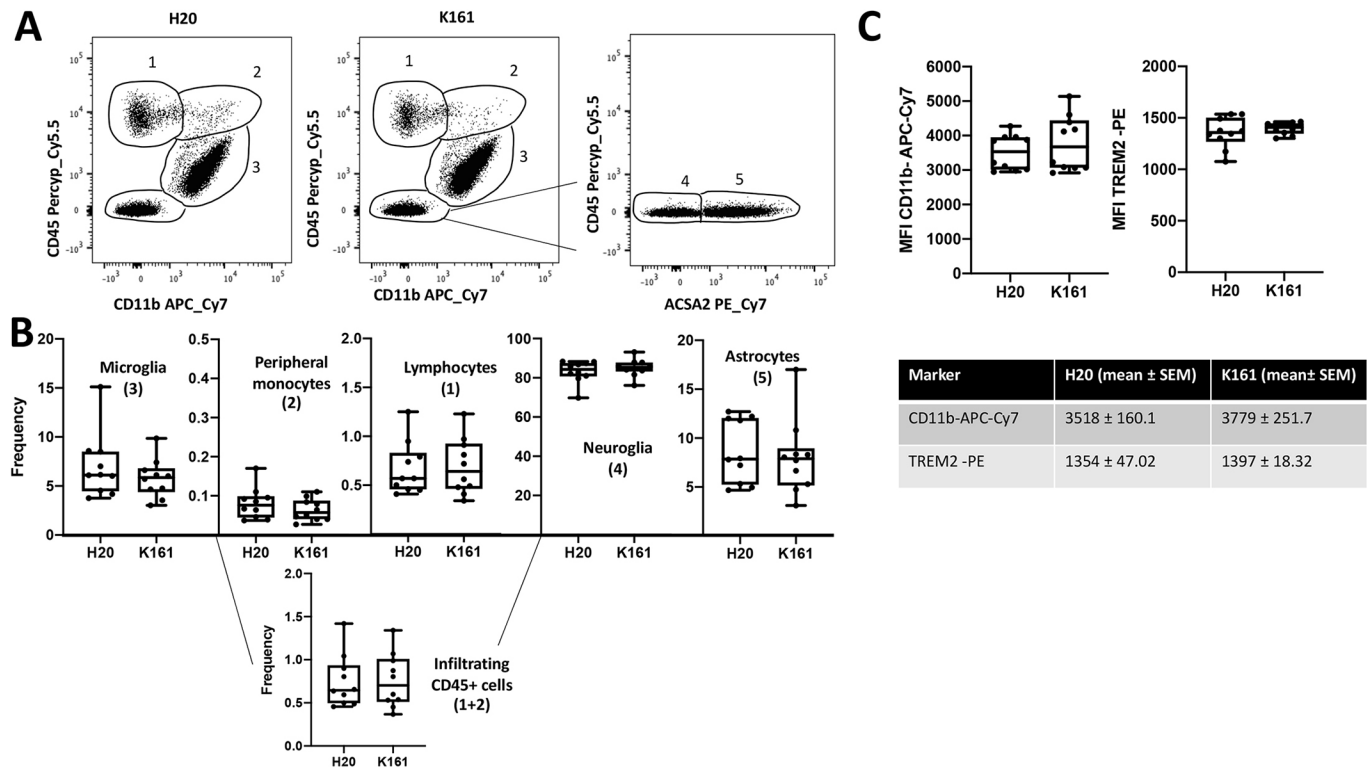


Fig. 7. Pan-SHIP1/2 inhibition *in vivo* does not alter the frequency of major cell populations in the cerebral cortex. (A,B) Single-cell suspensions of cerebral hemispheres were prepared from mice treated for 3 weeks (twice/week) with K161 (10 mg/kg) or vehicle and analyzed by flow cytometry ($n=10$ /group). (A) Representative contour plots of live gated single-cell populations 1–5, based on staining for CD11b, CD45 and/or ACSA2. (B) Box and whisker plots of frequency of the indicated cell population based on the gated populations 1–5 as defined in A, and total CNS-infiltrating CD45⁺ cells. (C) Scatter plots showing the mean fluorescence intensity (MFI) for CD11b and TREM-2 on CD11b⁺CD45^{low} microglia in K161-treated or vehicle-treated mice. The mean fluorescence intensity values and standard deviation of the mean for both CD11b and TREM2 in each group are provided below. Statistics: two-tailed *t*-test with Welch's correction. Error bars indicate min to max.

Given the prominent role SHIP1 has in macrophage and myeloid biology, it is surprising that the SHIP1-selective compound 3AC did not have a significant impact on basal signaling that limits phagocytic functions of microglia – particularly, since 3AC has compelling effects *in vitro* as well as *in vivo*. These include the ability to increase numbers of neutrophils and myeloid-derived suppressor cells (MDSCs; Brooks et al., 2010), and to induce G-CSF (Brooks et al., 2015) and osteoporosis (Iyer et al., 2014) – all of which are prominent phenotypes in SHIP1-deficient mice (Helgason et al.,

1998; Ghansah et al., 2004; Hazen et al., 2009; Takeshita et al., 2002; Iyer et al., 2014). The failure of SHIP1-selective 3AC to have a significant impact on microglia functions suggests that SHIP2 compensates for reduced SHIP1 activity in pathways that control lysosomal content and phagocytic function in microglia. Phagocytosis by macrophages is thought to require the SHIP1 and SHIP2 substrate PI(3,4,5)P₃ (Demirdjian et al., 2018), whereas PI(3,4,5)P₃ is essential for initial podosome formation with the target (Ostrowski et al., 2019). PI(3,4,5)P₃ also enables podosome

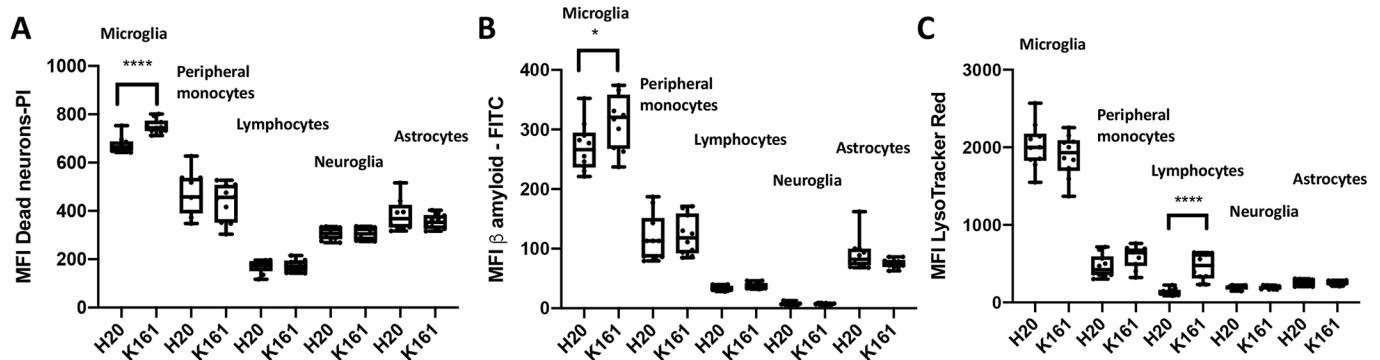


Fig. 8. Pan-SHIP1/2 inhibition *in vivo* increases the phagocytic capacity of microglia for both A β ₁₋₄₂ and dead neurons. (A–C) Single-cell suspensions of cerebral cortexes as described in Fig. 7 were used to measure uptake of A β ₁₋₄₂-FITC, dead PI-labeled neurons or staining of LysoTracker Red by using the assay conditions established for BV-2 cells and primary microglia. Box and whisker plots indicate the mean uptake of A β ₁₋₄₂-FITC (A), dead PI-labeled neurons (B) or staining with LysoTracker Red (C) for the indicated cerebral cortical cell population in either K161-treated or H₂O-treated mice after gating on live single cells, and surface markers CD11b, CD45 and/or ACSA2 as indicated. Statistical tests: Brown-Forsythe and Welch's ANOVA or two-tailed *t*-test with Welch's correction. * $P<0.05$, **** $P<0.0001$. Error bars indicate min to max.

formation in nascent phagocytic cups, enhancing binding to the phagocytic target and, thus, further facilitating probing of the target surface by exploratory lamellipodia (Ostrowski et al., 2019). Consistent with this role of PI(3,4,5)P₃, SHIP1 is known to limit phagocytosis by peripheral macrophages and degrades PI(3,4,5)P₃ present in phagosomes (Kamen et al., 2008, 2007). Consistent with SHIP1 and SHIP2 being recruited to the plasma membrane to control membrane invagination events triggered by surface-bound receptors, both can also promote a clathrin-independent form of receptor-mediated endocytosis called fast-endothelin-mediated-endocytosis through production of PI(3,4)P₂ (Boucrot et al., 2015). Because both SHIP1 and SHIP2 are co-expressed by macrophages and microglia, and known to be recruited to key macrophage receptors (e.g. FcγRIIb, M-CSF-R), they are both likely to be able to reduce basal PI(3,4,5)P₃ levels at the plasma membrane in microglia during initial phagocytic target engagement through PI3K-associated receptors (e.g. TREM2) (Segawa et al., 2017; Wang et al., 2004; Ono et al., 1996; Damen et al., 1996; Lioubin et al., 1996; Bruhns et al., 2000). Consistent with this hypothesis, both SHIP1 and SHIP2 are recruited to phagosomes and are involved in their formation and maturation, because Kamen et al. found that phagosomes in SHIP1^{-/-} macrophages have an increased ratio of PI(3,4,5)P₃:PI(3,4)P₂. However, importantly, the SHIP1 and SHIP2 product PI(3,4)P₂ was still present at significant levels, suggesting that SHIP2 is also present during phagosome formation in macrophages (Kamen et al., 2008). Thus, pan-SHIP1/2 inhibitors – through their combined action on both SHIP paralogs – may increase PI(3,4,5)P₃ levels at the plasma membrane to raise the efficiency of target engagement and phagocytic cup formation in microglia. This is an especially strong possibility for microglia, as both M-CSF and IL34 promote microglial survival in the CNS (Ginhoux et al., 2010; Kana et al., 2019; Greter et al., 2012; Alliot et al., 1999) and both SHIP1 and SHIP2 are recruited to M-CSF/IL34 receptor to limit production of PI(3,4,5)P₃ through PI3K (Lioubin et al., 1996; Damen et al., 1996; Wang et al., 2004). Thus, dual inhibition of both SHIP paralogs can potentially increase basal PI(3,4,5)P₃ levels at the plasma membrane of microglia, and might further enhance the efficiency of phagocytosis when microglia engage targets (e.g. dead neurons or Aβ deposits) to be phagocytosed through pattern recognition receptors (PRRs), such as TREM2 or dectin1.

One of the phagocytic functions we did not examine in this study is the ability of microglia to take up antibody–antigen complexes or immune complexes. This ability is not thought to be a homeostatic function of microglia as most antibody isotypes do not typically cross the blood-brain barrier and the CNS is generally considered an immune-privileged site. Nonetheless, anti-Aβ42 monoclonal antibodies have been developed and tested as therapeutics for Alzheimer's disease, but most did not demonstrate efficacy. However, a recent phase 2 trial of BAN2401 (Eisai Inc.), an anti-Aβ protofibril antibody, demonstrated reduced amyloid burden and delayed cognitive decline in Alzheimer's disease patients (EISAI Co. Ltd., 2019). Therefore, the pan-SHIP1/2 inhibitors we describe here might endow CNS-resident microglia with increased capacity to phagocytose amyloid deposits opsonized (i.e. made more susceptible to phagocytosis) by such therapeutics to increase their efficacy in Alzheimer's disease. Such an effect of pan-SHIP1/2 inhibitors need not to be restricted to FcγRs signaling, as the SHIP1-regulated microglial receptor TREM2 also promotes microglial clearance of opsonized amyloid plaques (Xiang et al., 2016).

Pan-SHIP1/2 inhibitory compounds – including K161 – can increase lysosomal capacity and proliferation of microglia cell lines

and primary neonatal microglia *ex vivo*. K161 was unable to increase lysosomal compartment size or the number of brain-resident microglia in the cerebral cortex *in vivo*. However, K161 did promote an increase in lysosomal compartment size in peripheral lymphocytes that trafficked to the CNS, indicating that it acts on cells in the brain to increase lysosomal capacity. The fact that neither the size of the lysosomal compartment nor microglial numbers were increased in the cerebral cortex might reflect that K161 was acting on a fully differentiated cell type within its native tissue location and under normal homeostasis – i.e. in the absence of a pathologic stressor. There are very likely to be other regulatory mechanisms that set strict limits on these two microglial parameters in young wild-type mice with normal physiology. We speculate, though, that – when the CNS is stressed by increased neuronal death, NFTs and/or Aβ-related pathology – pan-SHIP1/2 inhibitors alter microglial frequency in the CNS and/or their lysosomal capacity. In addition, the effects on myeloid and lymphoid cell populations infiltrating the brain in response to treatment with pan-SHIP1/2 inhibitors might be different in aged (12 to 24 months old) mice compared with young (2 to 6 months old) mice, as suggested by the fact that SHIP1-deficiency skews hematopoiesis towards an increased myelopoietic output when mice age (Iyer et al., 2015).

The role of microglia as being either beneficial or harmful in Alzheimer's disease and its progression remains controversial, as there are valid data to support either hypothesis (Sarlus and Heneka, 2017; Hansen et al., 2018; Colonna and Butovsky, 2017). There is mounting evidence that, when developing mild cognitive impairments or prodromal symptoms, which then progress into Alzheimer's disease with severe loss of cognition, microglia are placed under chronic rather than acute stress (Sarlus and Heneka, 2017; Hansen et al., 2018; Colonna and Butovsky, 2017). This prolonged activation *in vivo*, which results from continuous exposure to increased amyloid deposits and tau tangles, brings about substantial cellular changes in microglia – sometimes with the appearance of 'dark microglia' during progression to severe Alzheimer's disease (Bisht et al., 2016). In general, microglia are thought to become more inflammatory – rather than maintaining homeostasis or healing – when Alzheimer's disease progresses. However, SHIP inhibitors, like 3AC but also the pan-SHIP1/2 inhibitor K118, have been shown to promote an increase in the number and function of immunoregulatory macrophage populations, such as MDSCs and alternatively activated (M2) macrophages – both of which are capable of reducing inflammation and promoting tissue healing (Brooks et al., 2010). In fact, K118 was able to strongly bias macrophage differentiation in visceral adipose tissue towards the M2 macrophage type during ongoing inflammation induced by continued consumption of a high-fat diet. This suggests that, during disease progression, prolonged treatment with pan-SHIP1/2 inhibitors enables the microglial compartment to resist evolving into dark or inflammatory microglia with ongoing amyloid stress. Consistent with this possibility, dectin1 promotes the metabolic fitness of microglia (Ulland et al., 2017) and SHIP1 limits dectin1 signaling (Blanco-Menendez et al., 2015). However, stress-induced endogenous ligands in the CNS that might be recognized by dectin1 remain undefined. Nonetheless, dectin1 enables macrophage recognition of apoptotic cells (Weck et al., 2008) and, through binding to vimentin, also necrotic and senescent cells (Thiagarajan et al., 2013; Frescas et al., 2017). Others have recently reported that systemic signals can alter the composition of the microglial compartment to cells with a trained or more inflammatory capacity vs those with a tolerant or homeostatic function, with the latter proposed to be more beneficial for protection against dementia

(Wendeln et al., 2018; Keren-Shaul et al., 2017). We have shown that, by altering the selectivity of SHIP inhibitors and/or changing their treatment intensity (i.e. frequency of administration) we can boost tumor immunity (Gumbleton et al., 2017), improve immune resistance to a fungal challenge (Saz-Leal et al., 2018), reduce inflammation-mediated obesity (Srivastava et al., 2016) and compromise host rejection of a BM allograft (Fernandes et al., 2015). We anticipate that – depending on further optimization of which pan-SHIP1/2 inhibitors compound is used as well as duration and frequency of treatment, – it is possible to promote sustained microglial homeostatic function, even in the face of ongoing stress of amyloidosis.

Our findings provide the first demonstration that microglial homeostatic function can be enhanced pharmacologically *in vitro* and, importantly, *in vivo*. They suggest that simultaneous inhibition of the SHIP1 and SHIP2 paralogs provide a means to enhance basal microglial homeostatic function for therapeutic purposes in Alzheimer's disease and, possibly, other types of dementia where microglial homeostatic function is inadequate. Thus, pan-SHIP1/2 inhibitors may represent a novel immunotherapy to treat Alzheimer's disease.

MATERIALS AND METHODS

Mice

3-month-old C57BL/6J mice were purchased from Jackson Laboratories (Bar Harbor, ME) for *in vivo* studies of SHIP inhibitors described herein. Prior to and during *in vivo* studies, mice were housed at the SUNY Upstate Medical University vivarium under conventional, nonspecific-pathogen-free conditions. Animal experiments were approved by the Institutional Animal Care and Use Committee (IACUC) at SUNY Upstate Medical University.

Cells

The BV-2 and SIMA-9 microglial cell lines were purchased from the American Type Culture Collection (ATCC) and cultured following ATCC instructions. For flow cytometry assays cells were seeded at a density of 5×10^5 /ml.

Proliferation assay

Cells were seeded at 2×10^5 /ml. After 48 h of inhibitor treatment, cells were incubated for 1 h (BV-2) or 3 h (primary microglia) with the Cell Counting Kit-8 reagent CCK-8 (Dojindo Molecular Technologies); absorbance values were measured at 450 nm.

Western blots

All antibodies used for western blots were purchased from Santa Cruz: Actin (C-4), HSP90 α / β (F-8), SHIP1 (P1C1), SHIP2 (E-2). The secondary anti-mouse IgG κ -binding protein-HRP (Santa Cruz) was used to reveal the blotting. Conditions for western blot detection of SHIP1, SHIP2 and housekeeping controls have been described previously (Brooks et al., 2010; Fuhler et al., 2012; Hoekstra et al., 2016). All antibodies were used at concentration specified by the supplier.

Primary murine microglia preparation

Primary microglia cells were prepared from 2–8-day-old neonatal cerebrum and cultured up to 8 weeks following a waiting period of 1 week for the establishment of the cell culture as described by Bonaparte et al., 2006. To obtain cells enriched to ~95% for microglia from these mixed cell microglial–glial cultures, culture flasks were shaken at 150 rpm at 37°C for 30 min and supernatants filtered through 10- μ m strainers (BD) prior to seeding. When analyzed by flow cytometry, cells were gated on CD11b⁺CD45⁺ singlets that were DAPI⁻. This analysis routinely demonstrated that the viable cell suspension typically consisted of 95% CD45⁺CD11b⁺ microglia.

Intracellular staining for flow cytometric analysis

To perform intracellular staining of SHIP1 and SHIP2, cells were incubated with the viability stain of the Zombie Aqua Fixable Viability Kit (BioLegend),

fixed 20 min with IC Fixation Buffer (cat. number 00-8222-49, eBioscience), washed with permeabilization buffer (cat. number: 00-8333-56; eBioscience) and stained for SHIP1 (P1C1-A5 PE, dilution 1:100; BioLegend), SHIP2 (E-2 FITC, dilution: 1:100; Santa Cruz Biotechnology) in a final volume of 100 μ l. The same procedure was applied for intracellular staining of phosphorylated AKT at serine 472 (p-AKT AF488, clone M89-61, dilution: 1:20; Becton Dickinson). All surface and intracellular stains were performed in presence of species-specific Fc receptor blocking solution (TruStain-FcX cat.number 101320 BioLegend; Fc Receptor Binding Inhibitor, cat.number 14-9161-73 eBioscience.).

Analysis of lysosomal content

Cells were incubated with 50 nM LysoTracker Red DND-99 (Thermo Fisher) for 30 min. After a wash in PBS they were analyzed by flow cytometry or fixed for confocal microscopy. For confocal microscopy cells were seeded at 2×10^5 /ml in an eight-well Chamber Slide System (Thermo Fisher). After treatment, cells were stained, washed, fixed with 4% PFA for 20 min and mounted on glass coverslips in ProLong antifade mounting solution with DAPI (Thermo Fisher).

Differentiation of iPSC-derived hematopoietic progenitors to microglia

Hematopoietic stem/progenitor cells derived from the iPSC line (gift from Matthew Blurton-Jones, University of California, CA) were differentiated to microglia and other myeloid cell types using medium supplemented with M-CSF (25 ng/ml), IL34 (100 ng/ml) and TGF- β 1 (50 ng/ml) (Peprotech) for 2 weeks and adding CX3CL1 (100 ng/ml; Peprotech), CD200 (100 ng/ml; Novoprotein) for the third week (McQuade et al., 2018). The cells were then harvested and analyzed by FACS for the presence of microglia based on expression of human CD45. Uptake of apoptotic neurons was measured in this population of cells by flow cytometry. The iPS cell line UCI ADRC-5 and HPCs differentiated from them were provided by the University of California Alzheimer's Disease Research Center (UCI-ADRC) and the Institute for Memory Impairments and Neurological Disorders (Abud et al., 2017; McQuade et al., 2018).

Generation of dead neurons and analysis of dead neuron phagocytosis

Primary neurons were prepared from day 1–3 neonatal brains as described by Zhao et al. (2016). To induce apoptosis and to kill the neurons they were given 3200 Rads at 300 R/min for 640 s (32 Gy) from an X-ray source. Stocks of dead neurons stained with propidium iodide (PI) were prepared, diluted to 5×10^4 /ml and incubated for 2 h on microglial cells. After a wash in PBS, microglial cells were stained and analyzed by flow cytometry gating on a live, CD11b⁺ population. For confocal microscopy analysis, fixed cells were incubated for 30 min with blocking solution (PBS 3% FBS HI) and stained for 1 h with CD11b-AF488. Slides were then washed three times and mounted as previously described. Stocks of dead neurons were stored in the dark at 4°C for up to 4 weeks until used.

Analysis of A β ₁₋₄₂ phagocytosis

A β ₁₋₄₂-FITC (rPeptide) was incubated with microglial cells at 0.5 μ g/ml for 1 h and, after a wash with PBS, the sample was collected for flow cytometric analysis or confocal imaging.

Confocal imaging and quantification

All confocal images are representative of three z-stacks. For quantification proposes the central plane of the z-stacks was selected and mean fluorescence intensity of each cell was analyzed with Fiji software for 40–150 cells. Data were converted from bit to gray scale and reported in a dot plot graph for statistical analysis after elimination of outliers using Tukey's test.

Preparation of SHIP inhibitors

The known SHIP inhibitors used in this study are K149 (Sosič et al., 2015), 3AC (Brooks et al., 2010) and K118 (Brooks et al., 2015), which were prepared as previously described in the associated references. The protocols for preparation of novel SHIP1/2 inhibitors (K116, K161 and K185) used

here are available upon request. In addition, Table S1 lists the structures of all compounds used in this study and the IC₅₀ for both SHIP1 and SHIP2.

In vivo treatment of mice with K161

C57BL/6 mice (3 months old) were treated twice a week for 3 weeks by intra-peritoneal (i.p.) injection of either 10 mg/ml K161 in H₂O or vehicle control (H₂O). The exact dosage regimen used was similar to that used for K118 in an obesity model (Srivastava et al., 2016) and consisted of a single i.p. injection of K161 (10 mg/kg) administered on days 1, 4, 8, 11, 15 and 18. Mice were then killed on day 19 and their brains analyzed as described. The brains were collected after killing and perfusing the mice with cold PBS supplemented with 0.5% BSA. Brain dissociation was performed using the Miltenyi Neural Tissue Dissociation Kit (P) followed by removal of myelin. For the latter Miltenyi anti-myelin beads and AutoMACS separation was used. The cell suspension was then incubated with Aβ₁₋₄₂-FITC, dead neurons were labeled with PI or LysoTracker Red with the same procedure used for the cell lines described above. The cell suspension was then stained with surface stain for CD11b (BioLegend), CD45 (Biolegend), ACSA2 (Miltenyi), and DAPI or PI (for live or dead discrimination, respectively), and analyzed by flow cytometry. For intracellular staining of SHIP1 in CNS cell populations the same procedure as for cell lines was used.

LC-MS quantification of K161 in the CNS and serum

Serum proteins were precipitated by adding 120 μl of acetonitrile (ACN) to 20 μl of sample. Following centrifugation, the supernatant was recovered and dried under vacuum. The pellets were re-dissolved in 20 μl of 20% methanol (MeOH), 0.1% formic acid in water. External calibration curves were generated by pooling serum from non-treated animals, dividing it over six 20-μl aliquots, and by spiking each aliquot with 2.2 μl K161 to produce final concentrations of 30–10,000 nM. The standards were further processed as described above for treated serum samples. Weighed cerebrum samples were placed in tubes pre-filled with homogenizer beads (Omni International, 19-627). To each sample, approximately one volume of Tris-buffered saline (pH 7.6) containing 10% ACN was added. The samples were homogenized in a Bead Ruptor Elite (Omni International, 19-040E) at 4 m/s for three cycles of 15 s with a 30 s dwell between cycles. The homogenate was recovered into a new centrifuge tube, to which 1.0 ml of ACN was added. After 5 min, the samples were centrifuged, the supernatant collected and dried under vacuum. The pellets were re-dissolved in 200 μl of 20% MeOH, 0.1% formic acid in water. External calibration curves were generated by pooling brains from non-dosed animals, dividing this across six 50-μl aliquots, and spiking the aliquots with 5.5 μl of K161 to produce final concentrations of 30–10,000 nM. The standards were further processed as described above for treated brain samples. Of each sample or standard, 5 μl were injected onto a C18 column (2.1×30 mm, Interchim, UP30DB-030/021). A Vanquish UHPLC (Thermo Scientific) delivered a linear gradient from 20–95% B at 200 μl/min over 2.5 min, followed by a 4 min wash and re-equilibration. Solvents A and B were H₂O and methanol, respectively, both containing 0.1% formic acid. The LC was coupled to a Quantis Triple Quadrupole mass spectrometer (Thermo Scientific) operating in MRM mode with positive electrospray ionization (ESI) at 4000 V. The following transitions were monitored: m/z 291.4 to 274.2, 135.1, 147.1 and 161.1 with collision energies of 21–31 V and 75 ms dwell time per transition. Quantification was performed by using Thermo Xcalibur Quan Browser software.

Acknowledgements

W.G.K. is the Murphy Family Professor of Children's Oncology Research and an Empire Scholar of the State University of NY. We thank Dr Paul Massa for sharing expertise on the growth of primary murine microglia from neonatal brain. We are grateful to Mathew Blurton-Jones and Amanda McQuade (UCI-ADRC) for providing human iPS and differentiated hematopoietic progenitor cells used in this study, and for their generous advice on iPS growth and differentiation.

Competing interests

W.G.K., C.P., S.F. and J.D.C. have patents, pending and issued, concerning the analysis and targeting of SHIP1 and SHIP2 in disease. W.G.K. is Chief Scientific Officer and J.D.C. serves on the Scientific Advisory Board of Alterna Therapeutics,

which is devoted to developing and commercializing SHIP inhibitor therapeutics and hold equity. The other authors have no conflicts to disclose.

Author contributions

Conceptualization: C.P., W.G.K.; Methodology: C.P., O.D., S.D., D.V., A.A., L.C., E.D., J.C.; Formal analysis: C.P., S.F., E.D.; Investigation: C.P.; Writing - original draft: C.P., E.D., J.C., W.G.K.; Writing - review & editing: C.P., S.F., E.D., J.C., W.G.K.; Supervision: J.C., W.G.K.; Project administration: J.C., W.G.K.; Funding acquisition: J.C., W.G.K.

Funding

This work was supported in part by National Institutes of Health RO1 AG059717 and Pediatric Departmental support funds to C.P. and W.G.K. The UCI-ADRC is funded by National Institutes of Health/National Institute on Aging Grant P50 AG16573. Deposited in PMC for release after 12 months.

Supplementary information

Supplementary information available online at <http://jcs.biologists.org/lookup/doi/10.1242/jcs.238030.supplemental>

References

- Abud, E. M., Ramirez, R. N., Martinez, E. S., Healy, L. M., Nguyen, C. H. H., Newman, S. A., Yeromin, A. V., Scarfone, V. M., Marsh, S. E., Fimbres, C. et al. (2017). iPSC-derived human microglia-like cells to study neurological diseases. *Neuron* **94**, 278–293.e9. doi:10.1016/j.neuron.2017.03.042
- Alliot, F., Godin, I. and Pessac, B. (1999). Microglia derive from progenitors, originating from the yolk sac, and which proliferate in the brain. *Brain Res. Dev. Brain Res.* **117**, 145–152. doi:10.1016/S0165-3806(99)00113-3
- Bisht, K., Sharma, K. P., Lecours, C., Sánchez, M. G., EL Hajj, H., Milior, G., Olmos-Alonso, A., Gómez-Nicola, D., Luheshi, G., Vallières, L. et al. (2016). Dark microglia: A new phenotype predominantly associated with pathological states. *Glia* **64**, 826–839. doi:10.1002/glia.22966
- Blanco-Menendez, N., del Fresno, C., Fernandes, S., Calvo, E., Conde-Garrosa, R., Kerr, W. G. and Sancho, D. (2015). SHIP-1 couples to the dectin-1 hemiTAM and selectively modulates reactive oxygen species production in dendritic cells in response to *Candida albicans*. *J. Immunol.* **195**, 4466–4478. doi:10.4049/jimmunol.1402874
- Bonaparte, K. L., Hudson, C. A., Wu, C. and Massa, P. T. (2006). Inverse regulation of inducible nitric oxide synthase (iNOS) and arginase I by the protein tyrosine phosphatase SHP-1 in CNS glia. *Glia* **53**, 827–835. doi:10.1002/glia.20344
- Boucrot, E., Ferreira, A. P. A., Almeida-Souza, L., Debard, S., Vallis, Y., Howard, G., Bertot, L., Sauvonnet, N. and McMahon, H. T. (2015). Endophilin marks and controls a clathrin-independent endocytic pathway. *Nature* **517**, 460–465. doi:10.1038/nature14067
- Brooks, R., Fuhler, G. M., Iyer, S., Smith, M. J., Park, M.-Y., Paraiso, K. H. T., Engelman, R. W. and Kerr, W. G. (2010). SHIP1 inhibition increases immunoregulatory capacity and triggers apoptosis of hematopoietic cancer cells. *J. Immunol.* **184**, 3582–3589. doi:10.4049/jimmunol.0902844
- Brooks, R., Iyer, S., Akada, H., Neelam, S., Russo, C. M., Chisholm, J. D. and Kerr, W. G. (2015). Coordinate expansion of murine hematopoietic and mesenchymal stem cell compartments by SHIP1. *Stem Cells* **33**, 848–858. doi:10.1002/stem.1902
- Bruhns, P., Vély, F., Malbec, O., Fridman, W. H., Vivier, E. and Daëron, M. (2000). Molecular basis of the recruitment of the SH2 domain-containing inositol 5-phosphatases SHIP1 and SHIP2 by fcgamma R1IB. *J. Biol. Chem.* **275**, 37357–37364. doi:10.1074/jbc.M003518200
- Colonna, M. and Butovsky, O. (2017). Microglia function in the central nervous system during health and neurodegeneration. *Annu. Rev. Immunol.* **35**, 441–468. doi:10.1146/annurev-immunol-051116-052358
- Damen, J. E., Liu, L., Rosten, P., Humphries, R. K., Jefferson, A. B., Majerus, P. W. and Krystal, G. (1996). The 145-kDa protein induced to associate with Shc by multiple cytokines is an inositol tetraphosphate and phosphatidylinositol 3,4,5-triphosphate 5-phosphatase. *Proc. Natl. Acad. Sci. USA* **93**, 1689–1693. doi:10.1073/pnas.93.4.1689
- Demirdjian, S., Hopkins, D., Sanchez, H., Libre, M., Gerber, S. A. and Berwin, B. (2018). Phosphatidylinositol-(3,4,5)-Trisphosphate induces phagocytosis of nonmotile *Pseudomonas aeruginosa*. *Infect. Immun.* **86**. doi:10.1128/IAI.00215-18
- Dibble, C. C. and Cantley, L. C. (2015). Regulation of mTORC1 by PI3K signaling. *Trends Cell Biol.* **25**, 545–555. doi:10.1016/j.tcb.2015.06.002
- EISAI Co. Ltd. (2019). A study to evaluate safety, tolerability, and efficacy of BAN2401 in subjects with early Alzheimer's disease. <https://clinicaltrials.gov/ct2/show/NCT01767311>.
- El Khoury, J., Toft, M., Hickman, S. E., Means, T. K., Terada, K., Geula, C. and Luster, A. D. (2007). Ccr2 deficiency impairs microglial accumulation and accelerates progression of Alzheimer-like disease. *Nat. Med.* **13**, 432–438. doi:10.1038/nm1555

- Fernandes, S., Brooks, R., Gumbleton, M., Park, M.-Y., Russo, C. M., Howard, K. T., Chisholm, J. D. and Kerr, W. G. (2015). SHIPi enhances autologous and allogeneic hematopoietic stem cell transplantation. *EBioMedicine* **2**, 205-213. doi:10.1016/j.ebiom.2015.02.004
- Frescas, D., Roux, C. M., Aygun-Sunar, S., Gleiberman, A. S., Krasnov, P., Kurnasov, O. V., Strom, E., Virtuoso, L. P., Wrobel, M., Osterman, A. L. et al. (2017). Senescent cells expose and secrete an oxidized form of membrane-bound vimentin as revealed by a natural polyreactive antibody. *Proc. Natl. Acad. Sci. USA* **114**, E1668-E1677. doi:10.1073/pnas.1614661114
- Fuhler, G. M., Brooks, R., Toms, B., Iyer, S., Gengo, E. A., Park, M.-Y., Gumbleton, M., Viernes, D. R., Chisholm, J. D. and Kerr, W. G. (2012). Therapeutic potential of SH2 domain-containing inositol-5'-phosphatase 1 (SHIP1) and SHIP2 inhibition in cancer. *Mol. Med.* **18**, 65-75. doi:10.2119/molmed.2011.00178
- Ghansah, T., Paraiso, K. H. T., Highfill, S., Desponts, C., May, S., McIntosh, J. K., Wang, J.-W., Ninos, J., Brayer, J., Cheng, F. et al. (2004). Expansion of myeloid suppressor cells in SHIP-deficient mice represses allogeneic T cell responses. *J. Immunol.* **173**, 7324-7330. doi:10.4049/jimmunol.173.12.7324
- Ginhoux, F., Greter, M., Leboeuf, M., Nandi, S., See, P., Gokhan, S., Mehler, M. F., Conway, S. J., Ng, L. G., Stanley, E. R. et al. (2010). Fate mapping analysis reveals that adult microglia derive from primitive macrophages. *Science* **330**, 841-845. doi:10.1126/science.1194637
- Greter, M., Lelios, I., Pelczar, P., Hoeffel, G., Price, J., Leboeuf, M., Kundig, T. M., Frei, K., Ginhoux, F., Merad, M. et al. (2012). Stroma-derived interleukin-34 controls the development and maintenance of langerhans cells and the maintenance of microglia. *Immunity* **37**, 1050-1060. doi:10.1016/j.immuni.2012.11.001
- Griciuc, A., Patel, S., Federico, A. N., Choi, S. H., Innes, B. J., Oram, M. K., Cereghetti, G., McGinty, D., Anselmo, A., Sadreyev, R. I. et al. (2019). TREM2 acts downstream of CD33 in modulating microglial pathology in Alzheimer's disease. *Neuron* **103**, 820-835.e7. doi:10.1016/j.neuron.2019.06.010
- Guerreiro, R., Wojtas, A., Bras, J., Carrasquillo, M., Rogaeve, E., Majounie, E., Cruchaga, C., Sassi, C., Kauwe, J. S., Younkin, S. et al. (2013). TREM2 variants in Alzheimer's disease. *N Engl. J. Med.* **2**, 117-127. doi:10.1056/NEJMoa1211851
- Gumbleton, M., Sudan, R., Fernandes, S., Engelman, R. W., Russo, C. M., Chisholm, J. D. and Kerr, W. G. (2017). Dual enhancement of T and NK cell function by pulsatile inhibition of SHIP1 improves antitumor immunity and survival. *Sci. Signal.* **10**. doi:10.1126/scisignal.aam5353
- Hansen, D. V., Hanson, J. E. and Sheng, M. (2018). Microglia in Alzheimer's disease. *J. Cell Biol.* **217**, 459-472. doi:10.1083/jcb.201709069
- Hazen, A. L., Smith, M. J., Desponts, C., Winter, O., Moser, K. and Kerr, W. G. (2009). SHIP is required for a functional hematopoietic stem cell niche. *Blood* **113**, 2924-2933. doi:10.1182/blood-2008-02-138008
- Helgason, C. D., Damen, J. E., Rosten, P., Grewal, R., Sorensen, P., Chappel, S. M., Borowski, A., Jirik, F., Krystal, G. and Humphries, R. K. (1998). Targeted disruption of SHIP leads to hemopoietic perturbations, lung pathology, and a shortened life span. *Genes Dev.* **12**, 1610-1620. doi:10.1101/gad.12.11.1610
- Hickman, S. E. and El Khoury, J. (2010). Mechanisms of mononuclear phagocyte recruitment in Alzheimer's disease. *CNS Neurol. Disord. Drug Targets* **9**, 168-173. doi:10.2174/187152710791011982
- Hipolito, V. E. B., Ospina-Escobar, E. and Botelho, R. J. (2018). Lysosome remodelling and adaptation during phagocyte activation. *Cell. Microbiol.* **20**, 168-173. doi:10.1111/cmi.12824
- Hoekstra, E., Das, A. M., Willemsen, M., Swets, M., Kuppen, P. J. K., van der Woude, C. J., Bruno, M. J., Shah, J. P., ten Hagen, T. L. M., Chisholm, J. D. et al. (2016). Lipid phosphatase SHIP2 functions as oncogene in colorectal cancer by regulating PKB activation. *Oncotarget* **7**, 73525-73540. doi:10.18632/oncotarget.12321
- Hoskin, J. L., Sabbagh, M. N., Al-Hasan, Y. and Decourt, B. (2019). Tau immunotherapies for Alzheimer's disease. *Expert Opin. Investig. Drugs* **28**, 545-554. doi:10.1080/13543784.2019.1619694
- Hsieh, C. L., Koike, M., Spusta, S. C., Niemi, E. C., Yenari, M., Nakamura, M. C. and Seaman, W. E. (2009). A role for TREM2 ligands in the phagocytosis of apoptotic neuronal cells by microglia. *J. Neurochem.* **109**, 1144-1156. doi:10.1111/j.1471-4159.2009.06042.x
- Iyer, S., Viernes, D. R., Chisholm, J. D., Margulies, B. S. and Kerr, W. G. (2014). SHIP1 regulates MSC numbers and their osteolineage commitment by limiting induction of the PI3K/Akt/beta-catenin/Id2 axis. *Stem Cells Dev.* **23**, 2336-2351. doi:10.1089/scd.2014.0122
- Iyer, S., Brooks, R., Gumbleton, M. and Kerr, W. G. (2015). SHIP1-expressing mesenchymal stem cells regulate hematopoietic stem cell homeostasis and lineage commitment during aging. *Stem Cells Dev.* **24**, 1073-1081. doi:10.1089/scd.2014.0501
- Jay, T. R., Miller, C. M., Cheng, P. J., Graham, L. C., Bemiller, S., Broihier, M. L., Xu, G., Margevicius, D., Karlo, J. C., Sousa, G. L. et al. (2015). TREM2 deficiency eliminates TREM2+ inflammatory macrophages and ameliorates pathology in Alzheimer's disease mouse models. *J. Exp. Med.* **212**, 287-295. doi:10.1084/jem.20142322
- Jay, T. R., Hirsch, A. M., Broihier, M. L., Miller, C. M., Neilson, L. E., Ransohoff, R. M., Lamb, B. T. and Landreth, G. E. (2017). Disease progression-dependent effects of TREM2 deficiency in a mouse model of Alzheimer's disease. *J. Neurosci.* **37**, 637-647. doi:10.1523/JNEUROSCI.2110-16.2016
- Jiang, H., Liu, C. X., Feng, J. B., Wang, P., Zhao, C. P., Xie, Z. H., Wang, Y., Xu, S. L., Zheng, C. Y. and Bi, J. Z. (2010). Granulocyte colony-stimulating factor attenuates chronic neuroinflammation in the brain of amyloid precursor protein transgenic mice: an Alzheimer's disease mouse model. *J. Int. Med. Res.* **38**, 1305-1312. doi:10.1177/147323001003800412
- Jonsson, T., Stefansson, H., Ph, D. S., Jonsson, P. V., Snaedal, J., Bjornsson, S., Huttenlocher, J., Levey, A. I., Lah, J. J. et al. (2012). Variant of TREM2 associated with the risk of Alzheimer's disease. *N Engl. J. Med.* doi:10.1056/NEJMoa1211103
- Kamen, L. A., Levinsohn, J. and Swanson, J. A. (2007). Differential association of phosphatidylinositol 3-kinase, SHIP-1, and PTEN with forming phagosomes. *Mol. Biol. Cell* **18**, 2463-2472. doi:10.1091/mbc.e07-01-0061
- Kamen, L. A., Levinsohn, J., Cadwallader, A., Tridandapani, S. and Swanson, J. A. (2008). SHIP-1 increases early oxidative burst and regulates phagosome maturation in macrophages. *J. Immunol.* **180**, 7497-7505. doi:10.4049/jimmunol.180.11.7497
- Kana, V., Desland, F. A., Casanova-Acebes, M., Ayata, P., Badimon, A., Nabel, E., Yamamoto, K., Sneboer, M., Tan, I. L., Flanagan, M. E. et al. (2019). CSF-1 controls cerebellar microglia and is required for motor function and social interaction. *J. Exp. Med.* **216**, 2265-2281. doi:10.1084/jem.20182037
- Keren-Shaul, H., Spinrad, A., Weiner, A., Matcovitch-Natan, O., Dvir-Szternfeld, R., Ulland, T. K., David, E., Baruch, K., Lara-Astaiso, D., Toth, B. et al. (2017). A unique microglia type associated with restricting development of Alzheimer's disease. *Cell* **169**, 1276-1290.e17. doi:10.1016/j.cell.2017.05.018
- Kerr, W. G. (2011). Inhibitor and activator: dual functions for SHIP in immunity and cancer. *Ann. N. Y. Acad. Sci.* **1217**, 1-17. doi:10.1111/j.1749-6632.2010.05869.x
- Lambert, J.-C., Ibrahim-Verbaas, C. A., Harold, D., Naj, A. C., Sims, R., Bellenguez, C., Jun, G., DeStefano, A. L., Bis, J. C., Beecham, G. W., et al. (2013). Meta-analysis of 74,046 individuals identifies 11 new susceptibility loci for Alzheimer's disease. *Nat. Genet.* **45**, 1452-1458. doi:10.1038/ng.2802
- Li, B., Gonzalez-Toledo, M. E., Piao, C.-S., Gu, A., Kelley, R. E. and Zhao, L.-R. (2011). Stem cell factor and granulocyte colony-stimulating factor reduce beta-amyloid deposits in the brains of APP/PS1 transgenic mice. *Alzheimers Res. Ther.* **3**, 8. doi:10.1186/alzrt67
- Lioubin, M. N., Algate, P. A., Tsai, S., Carlberg, K., Aebersold, A. and Rohrschneider, L. R. (1996). p150Ship, a signal transduction molecule with inositol polyphosphate-5-phosphatase activity. *Genes Dev.* **10**, 1084-1095. doi:10.1101/gad.10.9.1084
- Mazzolla, R., Barluzzi, R., Brozzetti, A., Boelaert, J. R., Luna, T., Saleppico, S., Bistoni, F. and Blasi, E. (1997). Enhanced resistance to *Cryptococcus neoformans* infection induced by chloroquine in a murine model of meningoencephalitis. *Antimicrob. Agents Chemother.* **41**, 802-807. doi:10.1128/AAC.41.4.802
- Mcquade, A., Coburn, M., Tu, C. H., Hasselmann, J., Davtyan, H. and Blurton-Jones, M. (2018). Development and validation of a simplified method to generate human microglia from pluripotent stem cells. *Mol. Neurodegener.* **13**, 67. doi:10.1186/s13024-018-0297-x
- Moussa-Pacha, N. M., Abdin, S. M., Omar, H. A., Alniss, H. and Al-Tel, T. H. (2019). BACE1 inhibitors: current status and future directions in treating Alzheimer's disease. *Med. Res. Rev.* **35**, 19-24. doi:10.1002/med.21622
- Nagamoto-Combs, K., Kulas, J. and Combs, C. K. (2014). A novel cell line from spontaneously immortalized murine microglia. *J. Neurosci. Methods* **233**, 187-198. doi:10.1016/j.jneumeth.2014.05.021
- Nelson, P. T., Dickson, D. W., Trojanowski, J. Q., Jack, C. R., Boyle, P. A., Arfanakis, K., Rademakers, R., Alafuzoff, I., Attems, J., Brayne, C. et al. (2019). Limbic-predominant age-related TDP-43 encephalopathy (LATE): consensus working group report. *Brain* **142**, 1503-1527. doi:10.1093/brain/awz099
- Neumann, H. and Daly, M. J. (2012). Variant TREM2 as risk factor for Alzheimer's disease. *N Engl. J. Med.* doi:10.1056/NEJMe1213157
- Ono, M., Bolland, S., Tempst, P. and Ravetch, J. V. (1996). Role of the inositol phosphatase SHIP in negative regulation of the immune system by the receptor Fc(gamma)RIIB. *Nature* **383**, 263-266. doi:10.1038/383263a0
- Ostrowski, P. P., Freeman, S. A., Fair, G. and Grinstein, S. (2019). Dynamic podosome-like structures in nascent phagosomes are coordinated by phosphoinositides. *Dev. Cell* **50**, 397-410.e3. doi:10.1016/j.devcel.2019.05.028
- Parhizkar, S., Arzberger, T., Brendel, M., Kleinberger, G., Deussing, M., Focke, C., Nuscher, B., Xiong, M., Ghasemigharagoz, A., Katzmarski, N. et al. (2019). Loss of TREM2 function increases amyloid seeding but reduces plaque-associated ApoE. *Nat. Neurosci.* **22**, 191-204. doi:10.1038/s41593-018-0296-9
- Peng, Q., Malhotra, S., Torchia, J. A., Kerr, W. G., Coggshall, K. M. and Humphrey, M. B. (2010). TREM2- and DAP12-dependent activation of PI3K requires DAP10 and is inhibited by SHIP1. *Sci. Signal.* **3**, ra38. doi:10.1126/scisignal.2000500
- Prakash, A., Medhi, B. and Chopra, K. (2013). Granulocyte colony stimulating factor (G-CSF) improves memory and neurobehavior in an amyloid-beta induced experimental model of Alzheimer's disease. *Pharmacol. Biochem. Behav.* **110**, 46-57. doi:10.1016/j.pbb.2013.05.015

- Raben, N. and Puertollano, R. (2016). TFEB and TFE3: linking lysosomes to cellular adaptation to stress. *Annu. Rev. Cell Dev. Biol.* **32**, 255-278. doi:10.1146/annurev-cellbio-111315-125407
- Ruiz, A., Heilmann, S., Becker, T., Hernández, I., Wagner, H., Thelen, M., Mauleón, A., Rosende-Roca, M., Bellenguez, C., Bis, J. C. et al. (2014). Follow-up of loci from the International Genomics of Alzheimer's Disease Project identifies TRIP4 as a novel susceptibility gene. *Transl. Psychiatry* **4**, e358. doi:10.1038/tp.2014.2
- Sanchez-Ramos, J., Song, S., Sava, V., Catlow, B., Lin, X., Mori, T., Cao, C. and Arendash, G. W. (2009). Granulocyte colony stimulating factor decreases brain amyloid burden and reverses cognitive impairment in Alzheimer's mice. *Neuroscience* **163**, 55-72. doi:10.1016/j.neuroscience.2009.05.071
- Sanchez-Ramos, J., Cimino, C., Avila, R., Rowe, A., Chen, R., Whelan, G., Lin, X., Cao, C. and Ashok, R. (2012). Pilot study of granulocyte-colony stimulating factor for treatment of Alzheimer's disease. *J. Alzheimers Dis.* **31**, 843-855. doi:10.3233/JAD-2012-120196
- Sarlus, H. and Heneka, M. T. (2017). Microglia in Alzheimer's disease. *J. Clin. Invest.* **127**, 3240-3249. doi:10.1172/JCI90606
- Saz-Leal, P., del Fresno, C., Brandi, P., Martínez-Cano, S., Dungan, O. M., Chisholm, J. D., Kerr, W. G. and Sancho, D. (2018). Targeting SHIP-1 in myeloid cells enhances trained immunity and boosts response to infection. *Cell Rep.* **25**, 1118-1126. doi:10.1016/j.celrep.2018.09.092
- Segawa, T., Hazeki, K., Nigorikawa, K., Nukuda, A., Tanizawa, T., Miyamoto, K., Morioka, S. and Hazeki, O. (2017). Inhibitory receptor FcγRIIb mediates the effects of IgG on a phagosome acidification and a sequential dephosphorylation system comprising SHIPs and Inpp4a. *Innate Immun.* **23**, 401-409. doi:10.1177/1753425917701553
- Sly, L. M., Rauh, M. J., Kalesnikoff, J., Büchse, T. and Krystal, G. (2003). Ship, SHIP2, and PTEN activities are regulated in vivo by modulation of their protein levels: SHIP is up-regulated in macrophages and mast cells by lipopolysaccharide. *Exp. Hematol.* **31**, 1170-1181. doi:10.1016/j.exphem.2003.09.011
- Sosič, I., Anderluh, M., Sova, M., Gobec, M., Mlinarič Raščan, I., Derouaux, A., Amoroso, A., Terrak, M., Breukink, E. and Gobec, S. (2015). Structure-activity relationships of novel tryptamine-based inhibitors of bacterial transglycosylase. *J. Med. Chem.* **58**, 9712-9721. doi:10.1021/acs.jmedchem.5b01482
- Srivastava, N., Iyer, S., Sudan, R., Youngs, C., Engelman, R. W., Howard, K. T., Russo, C. M., Chisholm, J. D. and Kerr, W. G. (2016). A small-molecule inhibitor of SHIP1 reverses age- and diet-associated obesity and metabolic syndrome. *J. Clin. Invest. Insight* **1**, e88544. doi:10.1172/jci.insight.88544
- Suwa, A., Yamamoto, T., Sawada, A., Minoura, K., Hosogai, N., Tahara, A., Kurama, T., Shimokawa, T. and Aramori, I. (2009). Discovery and functional characterization of a novel small molecule inhibitor of the intracellular phosphatase, SHIP2. *Br. J. Pharmacol.* **158**, 879-887. doi:10.1111/j.1476-5381.2009.00358.x
- Takehita, S., Namba, N., Zhao, J. J., Jiang, Y., Genant, H. K., Silva, M. J., Brodt, M. D., Helgason, C. D., Kalesnikoff, J., Rauh, M. J. et al. (2002). SHIP-deficient mice are severely osteoporotic due to increased numbers of hyper-resorptive osteoclasts. *Nat. Med.* **8**, 943-949. doi:10.1038/nm752
- Taylor, C. A., Greenlund, S. F., McGuire, L. C., Lu, H. and Croft, J. B. (2017). Deaths from Alzheimer's disease - United States, 1999-2014. *MMWR Morb. Mortal. Wkly. Rep.* **66**, 521-526. doi:10.15585/mmwr.mm6620a1
- Thiagarajan, P. S., Yakubenko, V. P., Elson, D. H., Yadav, S. P., Willard, B., Tan, C. D., Rodriguez, E. R., Febbraio, M. and Cathcart, M. K. (2013). Vimentin is an endogenous ligand for the pattern recognition receptor Dectin-1. *Cardiovasc. Res.* **99**, 494-504. doi:10.1093/cvr/cvt117
- Tsai, K.-J., Tsai, Y.-C. and Shen, C.-K. (2007). G-CSF rescues the memory impairment of animal models of Alzheimer's disease. *J. Exp. Med.* **204**, 1273-1280. doi:10.1084/jem.20062481
- Ulland, T. K., Wang, Y. and Colonna, M. (2015). Regulation of microglial survival and proliferation in health and diseases. *Semin. Immunol.* **27**, 410-415. doi:10.1016/j.smim.2016.03.011
- Ulland, T. K., Song, W. M., Huang, S. C.-C., Ulrich, J. D., Sergushichev, A., Beatty, W. L., Loboda, A. A., Zhou, Y., Cairns, N. J., Kambal, A. et al. (2017). TREM2 maintains microglial metabolic fitness in Alzheimer's disease. *Cell* **170**, 649-663.e13. doi:10.1016/j.cell.2017.07.023
- van Dyck, C. H. (2018). Anti-amyloid-beta monoclonal antibodies for Alzheimer's disease: pitfalls and promise. *Biol. Psychiatry* **83**, 311-319. doi:10.1016/j.biopsych.2017.08.010
- Wang, Y., Keogh, R. J., Hunter, M. G., Mitchell, C. A., Frey, R. S., Javaid, K., Malik, A. B., Schurmans, S., Tridandapani, S. and Marsh, C. B. (2004). SHIP2 is recruited to the cell membrane upon macrophage colony-stimulating factor (M-CSF) stimulation and regulates M-CSF-induced signaling. *J. Immunol.* **173**, 6820-6830. doi:10.4049/jimmunol.173.11.6820
- Wang, Y., Cella, M., Mallinson, K., Ulrich, J. D., Young, K. L., Robinette, M. L., Gilfillan, S., Krishnan, G. M., Sudhakar, S., Zinselmeyer, B. H. et al. (2015). TREM2 lipid sensing sustains the microglial response in an Alzheimer's disease model. *Cell* **160**, 1061-1071. doi:10.1016/j.cell.2015.01.049
- Wang, Y., Ulland, T. K., Ulrich, J. D., Song, W., Tzaferis, J. A., Hole, J. T., Yuan, P., Mahan, T. E., Shi, Y., Gilfillan, S. et al. (2016). TREM2-mediated early microglial response limits diffusion and toxicity of amyloid plaques. *J. Exp. Med.* **213**, 667-675. doi:10.1084/jem.20151948
- Weck, M. M., Appel, S., Werth, D., Sinzger, C., Bringmann, A., Grünebach, F. and Brossart, P. (2008). hDectin-1 is involved in uptake and cross-presentation of cellular antigens. *Blood* **111**, 4264-4272. doi:10.1182/blood-2006-10-051375
- Wendeln, A.-C., Degenhardt, K., Kaurani, L., Gertig, M., Ulas, T., Jain, G., Wagner, J., Häsler, L. M., Wild, K., Skodras, A. et al. (2018). Innate immune memory in the brain shapes neurological disease hallmarks. *Nature* **556**, 332-338. doi:10.1038/s41586-018-0023-4
- Wimo, A., Guerchet, M., Ali, G.-C., Wu, Y.-T., Prina, A. M., Winblad, B., Jönsson, L., Liu, Z. and Prince, M. (2017). The worldwide costs of dementia 2015 and comparisons with 2010. *Alzheimers Dement.* **13**, 1-7. doi:10.1016/j.jalz.2016.07.150
- Xiang, X., Werner, G., Bohrmann, B., Liesz, A., Mazaheri, F., Capell, A., Feederle, R., Knuesel, I., Kleinberger, G. and Haass, C. (2016). TREM2 deficiency reduces the efficacy of immunotherapeutic amyloid clearance. *EMBO Mol. Med.* **8**, 992-1004. doi:10.15252/emmm.201606370
- Yoshino, Y., Yamazaki, K., Ozaki, Y., Sao, T., Yoshida, T., Mori, T., Mori, Y., Ochi, S., Iga, J.-I. and Ueno, S.-I. (2017). INPP5D mRNA expression and cognitive decline in Japanese Alzheimer's disease subjects. *J. Alzheimers Dis.* **58**, 687-694. doi:10.3233/JAD-161211
- Zhang, M., Schmitt-Ulms, G., Sato, C., Xi, Z., Zhang, Y., Zhou, Y., St George-Hyslop, P. and Rogava, E. (2016). Drug repositioning for Alzheimer's disease based on systematic 'omics' data mining. *PLoS ONE* **11**, e0168812. doi:10.1371/journal.pone.0168812
- Zhao, X., Zhang, L., Ting, S.-M. and Aronowski, J. (2016). Phagocytosis assay of microglia for dead neurons in primary rat brain cell cultures. *Bio. Protoc.* **6**. doi:10.21769/BioProtoc.1795

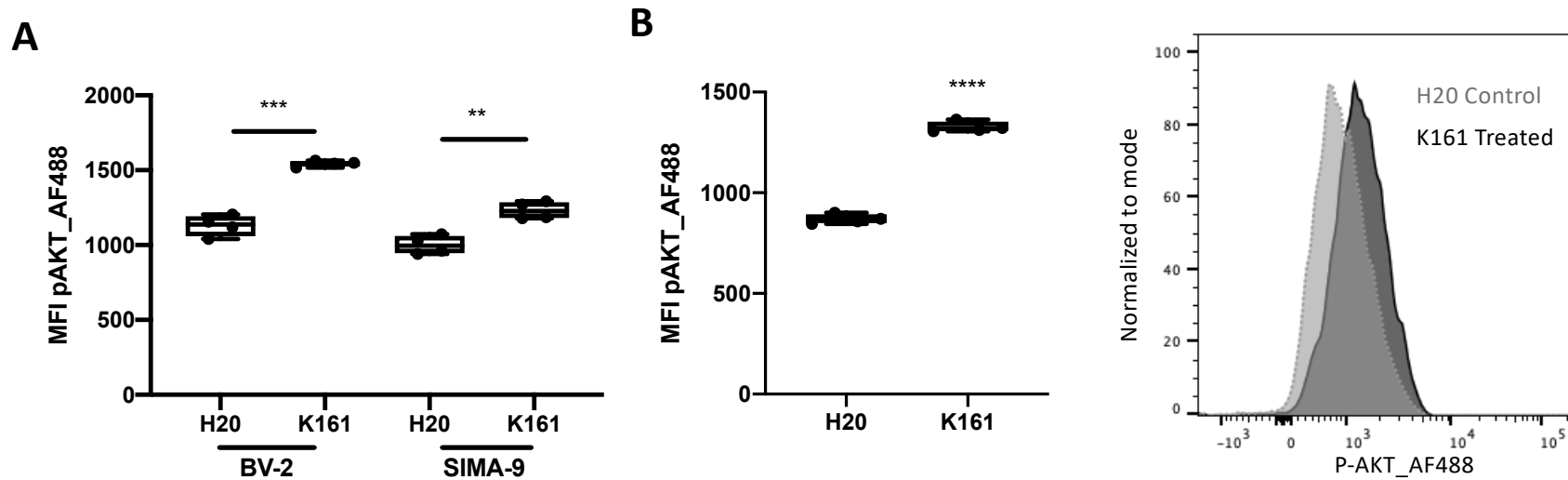


Figure S1. Pan-SHIP1/2 Inhibition induces AKT phosphorylation on serine 473. Box & whisker plots of p-AKT on (A) BV-2, SIMA-9 and (B) primary microglia with representative histogram for primary microglia K161 treated versus diluent control. Each plot is representative of three independent experiments and was analyzed with two-tailed T-test with Welch's correction (** $p < 0.01$, *** $p < 0.001$, **** $p < 0.0001$).

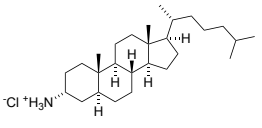
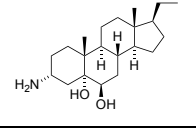
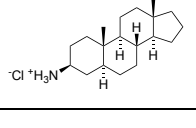
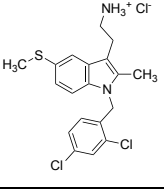
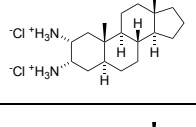
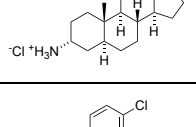
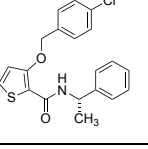
Compound	Structure	IC ₅₀ SHIP1 (μ M)	IC ₅₀ SHIP2 (μ M)	References
3AC (K100)		10	ND	(Brooks et al., 2010)
K116		1.5-6	6.5-13	-
K118		16	25	(Srivastava, 2016, Gumbleton et al., 2017)
K149		20-30	30	(Hoekstra et al., 2016)
K161		6	5-10	-
K185		18	30	-
AS1949490		13	0.6	(Suwa et al., 2009)

Table S1: Relative IC₅₀ and structures of inhibitory compounds for SHIP1 and/or SHIP2 enzyme activity based on a fluorescence polarization assay. ND, none detected (at 1mM by a Malachite Green assay of SHIP2 activity). (Brooks et al., 2010)